การสร้างเซ็นเซอร์เชิงแสงเพื่อการวิเคราะห์โลนิกเกิล (II)

นางสาวธัญพรรณ พลตื้อ

FABRICATION OF OPTICAL SENSOR FOR NICKEL (II) ANALYSIS

Miss Thanyapan Poltue

A Thesis Submitted in Partial Fulfillment of the Requirements
for the Degree of Master of Science Program in Chemistry
Department of Chemistry
Faculty of Science
Chulalongkorn University
Academic Year 2010

Thesis Title   FABRICATION OF OPTICAL SENSOR FOR NICKEL (II) ANALYSIS

By   Miss Thanyapan Poltue

Field of Study Chemistry

Thesis Advisor Luxsana Dubas, Ph.D.

Thesis Co-advisor Ratthapol Rangkupan. Ph.D.

Accepted by the Faculty of Science, Chulalongkorn University in Partial Fulfillment of the Requirements for the Master's Degree

…………………………………. Dean of the Faculty of Science

(Professor Supot Hannongbua, Dr.rer.nat.)

THESIS COMMITTEE

…………………………………. Chairman

(Assistant Professor Warinthorn Chavasiri, Ph.D.)

…………………………………. Thesis Advisor

(Luxsana Dubas, Ph.D.)

…………………………………. Thesis Co-advisor

(Ratthapon Rangkupan, Ph.D.)

…………………………………. Examiner

(Puttaruksa Varanusupakul, Ph.D.)

…………………………………. External Examiner

(Assistant Professor Anawat Pinisukul, Ph.D.)

ธัญพรรณ พลตื้อ : การสร้างเซ็นเซอร์เชิงแสงเพื่อวิเคราะห์โลหะหนัก. (FABRICATION OF OPTICAL SENSOR FOR HEAVY METAL ANALYSIS) อ.ที่ปรึกษาวิทยานิพนธ์หลัก: อาจารย์ ดร.ลักษณา ดูบาส, อ. ที่ปรึกษาวิทยานิพนธ์ร่วม: อาจารย์ ดร.รัฐพล รังกุพันธุ์, 82 หน้า.

การพัฒนาเซ็นเซอร์เพื่อตรวจวัดนิกเกิลในระดับความเข้มข้นต่ำด้วยตาเปล่า โดยการตรึงไดเมทธิลไกออกไซม์ซึ่งเป็นคัลลอริเมธทริกรีเอเจนต์ในแผ่นพอลิเมอร์รองรับ ได้แก่ เตรียมเส้นใยพอลีคาร์โปแลคโตนด้วยเทคนิคการปั่นเส้นใยด้วยไฟฟ้า, เตรียมแผ่นพอลีคาร์โปแลคโตนด้วยเทคนิคการฉาบ และการเตรียมแผ่นเจลาตินโดยเทคนิคการฉาบ และทำการเปรียบเทียบประสิทธิภาพในการตรวจวัดนิกเกิลของทั้งสามเทคนิค โดยศึกษาปัจจัยที่มีผลต่อการตรวจวัดนิกเกิลของเซ็นเซอร์เช่น อัตราส่วนโดยน้ำหนักที่เหมาะสมของไดเมทธิลไกออกไซม์และพอลีเมอร์ พีเอชของสารละลาย เวลาในการตอบสนอง รวมไปถึงไอออนรบกวน พบว่าเซ็นเซอร์นี้ตอบสนองต่อนิกเกิลไอออนโดยการเกิดเป็นสารประกอบเชิงซ้อนสีชมพูแดงของ $Ni(DMG)_2$ ที่พีเอช 9 ที่ความเข้มข้นของไอออนนิกเกิลต่างๆ โดยใช้เวลาในการตอบสนอง 10 นาที อัตราส่วนโดยน้ำหนักที่เหมาะสมของไดเมทธิลไกออกไซม์ต่อพอลีคาร์โปแลคโตน คือ 20 : 80 และอัตราส่วนโดยน้ำหนักที่เหมาะสมของไดเมทธิลไกออกไซม์ต่อเจลาตินคือ 3.6 : 96.4 โดยมีช่วงความเข้มข้นในการตอบสนอง 1-10 มิลลิกรัมต่อลิตร และขีดจำกัดของการตรวจวัดเท่ากับ 0.22, 0.18 และ 0.11 มิลลิกรัมต่อลิตร ของเซ็นเซอร์เส้นใยพอลีคาร์โปแลคโตน, แผ่นพอลีคาร์โปแลคโตนที่เตรียมด้วยเทคนิคการฉาบ และแผ่นเจลาตินที่เตรียมโดยเทคนิคการฉาบตามลำดับและเซ็นเซอร์ที่ได้มีความจำเพาะเจาะจงกับนิกเกิลมากกว่าไอออนรบกวน เช่น แคดเมียม แมงกานีส และโซเดียมที่ความเข้มข้นเดียวกัน นอกจากนี้ได้ทำการตรวจสอบประสิทธิภาพของระบบภายใต้การศึกษาปัจจัยต่างๆ โดยใช้สารละลายที่มีการเติมไอออนนิกเกิลเข้มข้น 1 และ 5 มิลลิกรัมต่อลิตร พบว่าให้ค่าร้อยละของการคืนกลับอยู่ในช่วง 104.4-105.0%, 102.6-104.7% และ 94.0-97.9% และค่าเบี่ยงเบนมาตรฐานสัมพัทธ์เท่ากับ 4.8 –6.2 %, 5.2-7.7% และ 5.0-7.4% ของเซ็นเซอร์เส้นใยพอลีคาร์โปแลคโตน, แผ่นพอลีคาร์โปแลคโตน และแผ่นเจลาตินตามลำดับ พบว่าสามารถนำเซ็นเซอร์ที่พัฒนาขึ้นนี้ไปประยุกต์ใช้ในการหาปริมาณของนิกเกิลที่มีความเข้มข้นต่ำในน้ำตัวอย่างได้

ภาควิชา ....เคมี........ ลายมือชื่อนิสิต ....

สาขาวิชา ....เคมี........ ลายมือชื่ออาจารย์ที่ปรึกษาวิทยานิพนธ์หลัก ....

ปีการศึกษา ....2553.... ลายมือชื่ออาจารย์ที่ปรึกษาวิทยานิพนธ์ร่วม ....

507 23034 23: MAJOR CHEMISTRY

KEYWORDS: POLY (CAPrOLACTONE) / GELATIN / DIMETHYGLYOXIME / NICKEL ION / ELECTROSPINNING / CASTING

THANTAPAN POLTUE: FABRICATION OF OPTICAL SENSOR FOR HEAVY METAL ANALYSIS. THESIS ADVISOR: LUXSANA DUBAS, Ph.D., THESIS CO-ADVISOR: RATTHAPOL RANGKUPAN, Ph.D., 82 pp.

The Low-cost optical polymer sensor was developed for the detection of nickel (II) ions in water based on immobilization of dimethylglyoxime (DMG) as a colorimetric reagent on polymer substrates. The sensors were fabricated by 3 different processes including polycaprolactone (PCL) doped with DMG electrospun fibers, PCL doped with DMG film and gelatin doped with DMG film. The critical parameters such as the mass ratio of DMG and PCL, pH of nickel solutions, response time and interference ions were studied. The sensor was responded to nickel (II) ions by forming red-pink color of $Ni(DMG)_2$ complex at pH 9. The optimum mass ratio of DMG and polymer media was found to be 20:80 for PCL/DMG electrospun fiber and film and 3.6:96.4 for gelatin/DMG film. All sensors showed the short response time of 10 minutes. The sensor was provided the response in range of 1-10 mg L^{-1} with detection limit of 0.22, 0.18 and 0.11 mg L^{-1} of PCL/DMG electrospun fiber, PCL/DMG film and gelatin/DMG film sensor, respectively. Both of PCL sensors expressed the good selectivity toward nickel(II) ions over cadmium (II), manganese(II) and sodium ions when present at equal concentration. Under the optimum conditions, the accuracy and precision of all sensors were investigated by using spiked water sample with standard nickel (II) solution at two concentration levels (1 and 5 mg L^{-1}).The recovery percentages were 104.4-105.0%, 102.6-104.7% and 94.0-97.9% for PCL/DMG fiber, PCL/DMG film and gelatin/DMG film sensor, respectively. The good precisions in range of 4.8-7.4% were attained for all sensors. The proposed method could be effectively applied for the determination of trace levels of nickel (II) ions in real water samples.

Department: …….Chemistry…… Student's Signature ....
Field of Study: …Chemistry…... Advisor's Signature ....
Academic Year: …….2010…..… Co-Advisor's Signature...

ACKNOWLEDGEMENTS

CONTENTS

LIST OF TABLES

LIST OF FIGURES

LIST OF ABBREVIATIONS

cm	=	Centimeter
^{o}C	=	Degree celcius
DMG		Dimethyglyoxime
F(R)		The Kubelka-Munk function
g	=	Gram
kV	=	Kilovolt
M	=	Molar concentration
ppm	=	Part per million
min	=	Minute
mL	=	Milliliter
µL	=	Microliter
mm	=	Millimeter
nm	=	Nanometer
PCL	=	Polycaprolactone
%RSD	=	Relative standard deviation percentage
S	=	Semen
SD	=	Standard deviation
SEM	=	Scanning electron microscope
TGA	=	Thermo gravimetric analysis
wt/v	=	Weight by volume
wt/wt	=	Weight by weight

CHAPTER I

INTRODUCTION

Nowadays many countries are encountering the environmental problems especially water pollution. The contamination of heavy metals in water is harmful to human, animals and plants. Among the widespread used heavy metals, nickel is a common toxic substance used in storage batteries, medal jewelry of nickel alloy and coil industry[1]. Nickel is a toxic metal and known to cause dispneumonitis, asthma, cancer of lungs, and disorder of respiratory and center of nervous system [2]. Due to its high toxicity, the Ministry of Science Natural Resources and Environment of Thailand set the guidelines and regulations for the maximum allowable nickel concentration in wastewater discharged from industries as 1.0 mg L^{-1}[3]. Furthermore, the concentration of Nickel in the environment should be regularly monitored. A number of method, such as atomic absorption spectroscopy (AAS) [4], inductively couple plasma atomic emission spectrometry (ICP-AES)[5] and inductively couple plasma mass spectrometry (ICP-MS)[6] can be used to determine nickel concentration. However, these methods generally require expensive instruments. Therefore, there is a critical need for the development of a simple, portable and inexpensive diagnostic tool to determine the amount of nickel (II) ions in field.

Optical sensor have played an important role in industrial, environmental and clinical monitoring since their introduction more than two decades ago as a result of their low cost, possibility for miniaturization and great flexibility. They also were used to successfully measure several heavy metal ions in water such as Cu^{2+}[7], Pb^{2+}[8], Hg^{2+}[9] and Ag^{+}[10]. In general, these sensors are comprised of various reagents immobilized on suitable membranes. A number of existing optical sensors utilize colored complexation between immobilized ligands and heavy metals. Most of previous works use colorimetric reagents such as dimethyglyoxime (DMG)[11], nioxime[12], 2(5-bromo-2-pyridylazo)-5-(dimethylamino)phenol[13], thionine[14] and 2-amino-1-cyclopentene-1-dithiocarboxylic acid[15] for determination of nickel

ions in water sample. However, all of these methods require instruments and sample pretreatment steps for nickel determination. According to our knowledge, there is no study shown the sensor that can measure nickel in simple step as dipping sensor into water samples and can be used in the field. Therefore, the development and fabrication of sensors for detecting nickel in simple step and in the field are great contemporary interest.

Among many types of colorimetric reagent, DMG is the one of most selective reagent for nickel. DMG reacts with nickel to form a red-pink complex which can be directly observed by visual detection. Thus, DMG was used as colorimetric reagent in this work. Electrospinning and casting methods were the choice of the sensor fabrication processes. Casting is conventionally process for preparing thin membranes. This process shows the advantage, which is simple and easy to operate. Electrospinning process can be produced the polymer fibers with diameter ranging from several micrometers (e.g. 10-100 μm) to sub-micrometer or nanometer (e.g. 10×10^{-3}-100×10^{-3} μm)[16]. The fibers show the several characteristics such as very large surface area per volume ratio (10^3 times of fiber)[17], flexibility in surface functionalities, and superior mechanical performance[18].

In this work, we demonstrated the colorimetric sensor for measuring nickel by using polymer containing DMG as sensing materials. Sensors were fabricated by electrospining and casting technique. It can be used as a novel optical sensor for the analysis of nickel ions concentration by simply dipping into the solution. The optical response of the sensor is based on the well know reaction between nickel and DMG leading to the formation of a red complex of $Ni(DMG)_2$ with an absorbance peak at 550 nm. The prepared substrate displayed a good color change when exposed to a various concentration of nickel solutions as low as few ppm of nickel in water.

1.1 Research Objective

The objective of this work is to develop the sensor for nickel determination by using DMG as colorimetric reagent immobilized on polymer films and fibers.

1.2 Scope of the Research

The scope of this research includes:

1) Fabrication of optical sensor by immobilizing DMG into different substrate such as Gelatin films, Polycaprolactone (PCL) films and PCL fibers.

2) Characterization of the optical sensors.

3) Study the influence of several parameters on the sensor performance such as amount of DMG, pH of solution, response time and interfering ions.

4) Method Validations; the detection limit, accuracy, precision, repeatability and reproducibility.

5) Application of the proposed method to real water sample analysis.

1.3 Benefits of the Research

This research aimed to obtain a portable, simple step and inexpensive optical sensor for determination of nickel ions in water samples.

CHAPTER II

THEORY AND LITERATURE REVIEWS

2.1   Heavy metals in the environment

Heavy metals are one group of pollutants in the environment that are harmful to human and animal due to their toxic effects. This research focuses on the analysis of nickel that is a toxic metal and harmful to human even at a very low contamination level.

Nickel is a one of heavy metal that occurs in the environment only at very low levels. Nickel was used for many different applications. The most common application is the use as an ingredient of steal and other metal products. It can be found in common metal products such as jewelry, nickel steels and nickel alloy [1]. Nickel can also end up in surface water when it is a part of wastewater streams. Nickel may be introduced into humans by breathing air, drinking water, eating food or smoking cigarettes. Skin contact with nickel-contaminated soil or water may also result in nickel exposure. In small quantities nickel is essential, but when the uptake is too high it can be a danger to human health. It affects on chances of development of lung cancer, nose cancer, larynx cancer and prostate cancer. It also causes heart disorders, lung embolism and respiratory failure [2]. Due to its toxicity, there are regulations on the permitted concentration of nickel in water sample. The allowable concentration of nickel in ground water set by the Ministry of Natural Resources and Environment is 0.1 mg L^{-1} [3]. The wastewater from the industries quality standards are shown in Table 2.1. The determination of nickel concentration in environmental sample water was required.

Table 2.1 Guidelines and maximum permitted levels of heavy metal in discharged industrial effluent water in Thailand [3]

Elements	Maximum acceptable concentration (mg L^{-1})
Zinc (Zn)	5.0
Lead (Pb)	0.2
Arsenic (As)	0.25
Selenium (Se)	0.02
Mercury (Hg)	0.05
Cadmium (Cd)	0.03
Cupper (Cu)	2.0
Nickel (Ni)	1.0
Barium (Ba)	1.0
Manganese (Mn)	1.0

2.2 Determination of nickel in water samples

The most commonly used techniques for nickel determination are spectrometric techniques, for example, atomic absorption spectroscopy (AAS) [4], inductively couple plasma atomic emission spectrometry (ICP-AES) [5], inductively couple plasma mass spectrometry (ICP-MS) [6] and anodic stripping voltammetry (ASV) [19]. While AAS and photometry are single element methods, ICP-AES and ICP-MS are used for multi-element analysis.

These methods present good detection limit and wide linear ranges, but require high cost analytical instruments developed for the use in the laboratories. The necessary collection transportation and pretreatment of a sample is time consuming and a potential source of error [20]. Therefore, the development of optical sensors for nickel determination was interested. Optical sensors enable to use in the field, thus, it can be actually a useful alternative tool [21].

2.3   Optical sensor

In this part, optical sensor is described as a small device which is able to responding to the presence of a heavy metal ion. The components of optical sensor device consist of (1) the recognition element that specific interaction with analyte, (b) the transducer element that converts the recognition process into a measurable optical signal and finally (c) a detector, which detects and converts the change of optical properties [21]. The optical properties of a material may be measured by the simply methods of absorbance, fluorescence and reflectance spectroscopy, and in different formats such as test strips and disposable tips. From the different reorganization process of optical sensor can generated the different sensors such as sensors based on intrinsic optical properties, sensors based on chromophores, sensors based on fluorophores, sensors based on ionophores, sensor based on enzyme inhibition along with sensor based on colorimetric reagent [22].

2.3.1 Schemes of optical sensor [23].

(a) Sensors based on the intrinsic optical properties of analytes

This sensor not based on the use of indicators but rather rely on the intrinsic optical properties of heavy metal ions, quantification are occurred by measuring of absorption or luminescence. Most of sensor configurations have been proposed including cells for absorbance measurements and single fiber, fiber bundle and fight-angle fiber configurations for fluorescence measurements.

(b) Sensors based on conventional chromogenic and fluorogenic reagents

Conventionally, heavy metal ions have been determined by using indicator dyes to binding with ions, especially of multiple charges. This reaction is accompanied by a change in the absorption or fluorescence of such chelators. In other words, an indicator acts as a transducer for the chemical species that cannot be determined directly by optical means.

(c) Sensors based on ionophores

Because of limitations of conventional reagents (mainly caused by their high stability constants) there has been an increase in the use of ionophores in optical chemical sensors. Ionophores are non-coloured ion-complexing organic molecules, or lipophilic ion carriers, which are capable of reversibly binding to ions and transporting them across organic membranes by carrier translocation.

(d) Sensor based on enzyme inhibition

Biosensors make use of biomolecules in the recognition or transduction process of sensors. While not obviously useful for sensing inorganic species, they have recently found application because of the interaction of heavy metal ions with certain proteins such as enzymes. In fact, specific and selective binding of metals to biomolecules offers tremendous possibilities in terms of selectivity and limits of detection.

2.3.2 Colorimetric sensor

Colorimetric sensor is an optical sensor device based on complexation between colorimetric reagent and metal ions. A large number of metal indicators exist containing various groups with electron donating atoms for binding [24]. Upon binding with the metal ion, most indicators undergo a change in color. Color changes, as signaling an event detected by the naked eye, are widely used owing to the low cost or lack of equipment required. A prominent example is Xylenol orange [25]. The EDTA-type complexing agent undergoes different color changes on binding metal ions[26] .

Dimethylglyoxime (DMG, $C_4H_8O_2N_2$) is the excellent complexing reagent for nickel ions and has been reported as one of the key reagent for sensing nickel ions by forming red complex of Ni-DMG$_2$[27]. The red complex can absorb the visible light at 550 nm. Various types of optical sensors were developed to determine nickel (II) ions in trace analysis such as using colorimetric solid phase extraction [28] and optical waveguide sensor [29]. The structure of Ni-DMG$_2$ complex was shown in Figure 2.1.
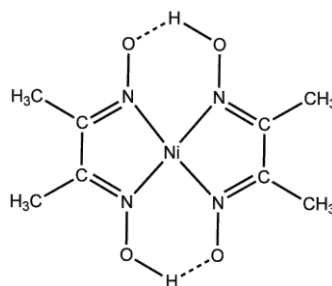
Figure 2.1 Structure of Ni(DMG)$_2$ complex

2.3.3 Polymeric supports

In sensor applications, indicator dyes and reagents are mostly used in immobilized form. The selection of polymer material has effected on performance of sensor [30]. For example, the response time of a sensor is occurred under the diffusion coefficients of ions in the polymer. Various heavy metal sensors, polymers are mostly prepared in thin membrane or film format. Because of the different polymer properties, it produced the membrane in different appearance: micro porous, fine porous, and non-porous or bulk membranes, which affects differently on the sensor performance. Typical of polymer supported such as ion exchange resin [31], sol-gel glass [25], cellulose acetate [15] as hydrophilic supports and poly (vinyl chloride) [32] as hydrophilic support were used to optical sensor. Therefore, the selection of polymer as media of sensors is important to the sensor performance.

a) Hydrophilic supports [23]

Hydrophilic supports are characterized by a large number of hydrogen functions such as hydroxyl or amino, or by a large number of charged groups such as carboxy (COO$^-$) or sulfo (SO$_3^-$) on the polymer chains. It shows hydrophilic properties such as water soluble, swell in water and water penetration. Numerous examples of hydrophilic polymer support are the polysaccharides (cellulose), polyglycols, polyacylate and variety of so-called hydrogels.

Gelatin is the choice of hydrophilic support [33]. It is a product of the structural and chemical degradation of collagen. The structure of gelatin is shown in Figure 2.2 [34]. The important properties of gelatin are water soluble, swell in water,

amphoteric polymer, reversible sol-gel conversion, film forming and transparence solution. For film forming, a gelatin solution is spread in a thin layer over a surface and passes from a sol to a gel, it forms a transparence film [35].
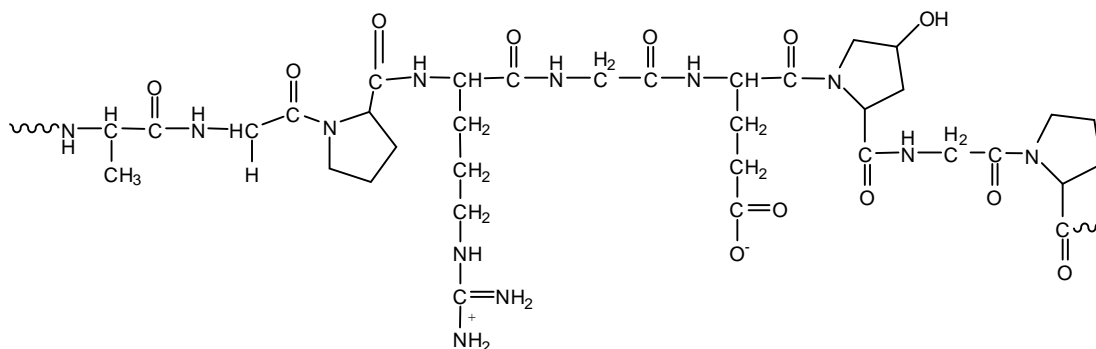
Figure 2.2 The structure of gelatin macromolecule

b) Hydrophobic supports

Hydrophobic properties are well known to be enhanced by an increased surface roughness [36], and super-hydrophobic surfaces require appropriate surface roughness and low surface energy. In contrast to hydrophilic supports, a clear separation exists between aqueous sample phase and the hydrophobic reagent phase. More recently, poly(vinyl choride) (PVC) have been used as hydrophobic supports for optical sensor based on ionophores. PVC is popular polymer for optical ions sensing because of certain cationic dyes can aggregate in PVC solution unless combined with a lipophilic counterion, an even distribution of the dye inside a membrane.

Poly(caprolactone) (PCL) is popular used as the hydrophobic supports [[37]. The structure of PCL is shown in Figure 2.2 [38]. PCL is biodegradable polymer with a low melting point and a low glass transition temperature. It is rubbery at room temperature, which contributes to the very high permeability of PCL for many chemical substances. PCL is widely used for drug delivery; drug compounds and tissue engineering scaffolds. It can form in many formats such as film, fiber and mesh. However, PCL is clearly white polymer that easy to detect when the optical properties of it are changed. As a result of PCL properties, it suitable for use as optical sensor.
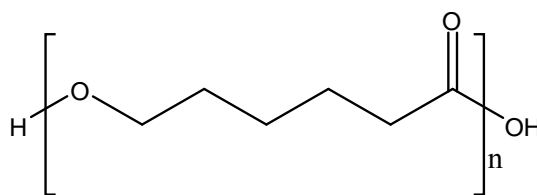
Figure 2.3 The structure of poly(caprolactone)

2.4 Diffuse reflection [39]

The optical phenomenons that usually measured the changing optical property of optical sensor are absorbance, fluorescence and reflectance.

The optical phenomenon known as diffuse reflectance is commonly used in the UV-visible, near-infrared and mid-infrared regions, especially of a matte surface such as inorganic powders. A reflectance spectrum is obtained by the collection and analysis of surface-reflected electromagnetic radiation as a function of frequency (v. usually in wavenumbers, cm^{-1}). Two different types of reflection can occur; regular or specular reflectance usually associated with reflection from smooth, polished surface like a mirrors, and diffuse reflection associated with reflection from so-called mat or dull surfaces textured like a powders. Regular and diffuse reflections are shown in Figure 2.4
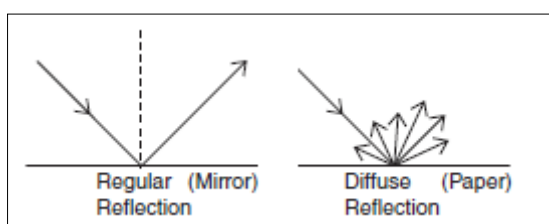
Figure 2.4 The pattern of regular and diffuse reflection

From figure 2.4, a flat surface reflects light at an angle equal to the incident angle of the light. This kind of reflection is called regular reflection. Surface roughness causes diffuse reflection. When the roughness has a regularly repeating pattern, with pattern separation on the same order of incident light, the resulting phenomena is diffuse reflection. The most often used theory to describe and analyze

diffuse reflectance is the Kubelka-Munk theory. The Kubelka-Munk, *F(R)*, is defined as:

$$F(R) = \frac{(1-R)^2}{2R}$$

Where *R* is percent reflectance measured with respect to a standard white. *F(R)* can be related to analyte concentration by [35].

$$F(R) = \frac{2.303\varepsilon C}{s}$$

Where *ε* is absorbtivity, *C* is the concentration of complexed analyte and *s* is the scattering coefficient of sample surface constant of the sample surface. By assuming the absorbtivity and scattering coefficient of surface are constant at a given wavelength, So, *F(R)* can be related directly to analyte concentration.

2.5 Sensor fabrication

The polymer film can fabricated in various techniques such as casting, spin-coating, dip-coating and drop-coating techniques [36]. Polymeric nanofiber is also fabricated in different technique. A number of techniques are available such as drawing, template synthesis, phase separation and electrospinning. In this study, we described about only selected techniques include of casting for preparation of polymer film and electrospinning for preparation of polymer fiber.

2.5.1 Casting technique

Conventionally, a film casting process is used to produce thin membranes. The process operated by the polymer solution is poured into substrate, and then allowed to solidify by evaporating of solvent. The solidified part is also known as a casting, which is ejected from the substrate to complete the process. The thickness of the film can be controlled during casting process.

2.5.2 Electrospinning technique

Electrospinning or electrostatic spinning is a technique use to describe a class of fiber forming process which electrostatic forces are employed to control the production of polymer fibers. Conventional fiber spinning techniques, e.g. melt spinning, dry spinning or wet spinning, rely on mechanical forces to produce fibers by extruding polymer melt or solution through a subsequently draw the resulting filaments as they solidify. Electrospinning offers a basically different approach to fiber production by introducing electrostatic forces to modify the fiber formation process. So, it can generate fiber in ranging of diameter from sub-micrometers down to nanometers. Due to the high surface area to volume ratio, high porosity, very small size, and light weight of the electrospun fibrous, they have favorable for many applications such as tissue engineering scaffolds, filtration devices, sensor, highly efficient filtration membranes, nanowires, nanocomposites and electrical materials [16]. In the process, a high voltage power supply is used to charge a polymer solution or melt through a metal contact, normally a needle, across a metal collection screen. The applied potential is in the range of 5 to 30 kV, depending on the collection distance. A reservoir containing a polymer solution or melt is attached to the metal contact with the small opening. When the polymer solution or melt is charged, the Coulombic repulsion force destabilizes the hemi spherical pendant droplet located changes in to a conical shape, which normally terms "the Taylor's cone" Further increase in the applied potential causes a charged jet to be ejected from the tip of the Taylor's cone. At right condition, fiber is formed as a result [25].

2.5.2.1 Electrospinning setup

Electrospining setup is preformed with 3 part of a basic apparatus. The experiment setup is shown in Figure.2.5

a) High voltage supply was used to charge the as-prepared polymer solutions between the needle (emitting electrode) and the collection screen (collecting electrode). It can generate electric potential in range of 0 to 30 kV.

b) Reservoir can be anything from a pipette to a syringe. Syringe pump is use to control the flow rate of the polymer solution, a 1-10 mL disposable syringe with hypodermic needle and connected to high voltage power supply.

c) Collector is performed with the rotator attached to aluminium foil or sieve of different geometry.
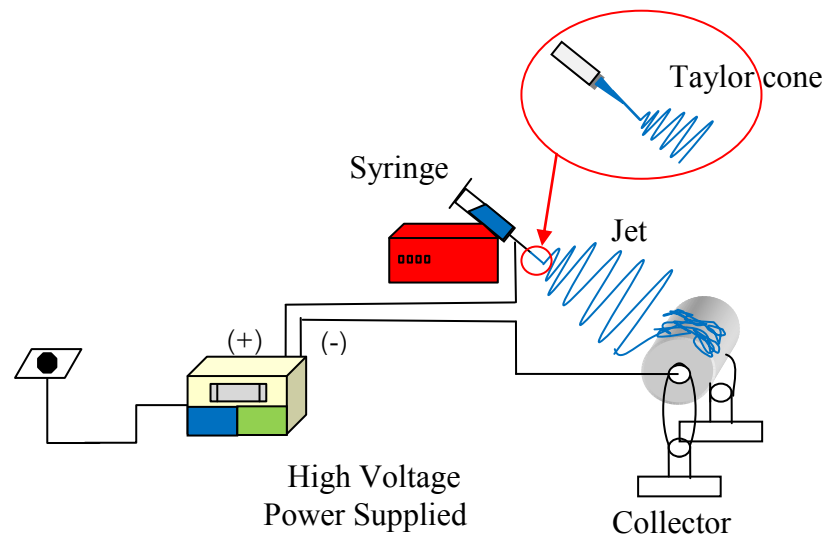
Figure 2.5 Schematic of the electrospinning process.

2.5.2.2 Basic principles of electrospinning [40]

Formation of fiber by electrospinning process, it creates nanofibers through an electrically charged jet of polymer solution or polymer melts. When the polymer solution or melt is charged, the polymer is ejected from a needle with forms a continuous nanofiber when the electrical force (due to the high electric potential of the polymer solution) overcomes the surface tension. At this point the pendant droplet of the polymer solution at the tip of the needle is deformed into conical shape, typically referred to as "Taylor cone". When the critical voltage is exceeded, the electrical force overcomes the surface tension and a fine charged jet is ejected. After the jet flows away from the droplet in a nearly straight line, it blends into a complex path and other changes in shape occur, during which electrical forces stretch and thin it by very large ratios. After the solvent gradually evaporates solid nanofibers are

form as nonwoven fabrics. The formation model of the Taylor cone is shown in Figure 2.6
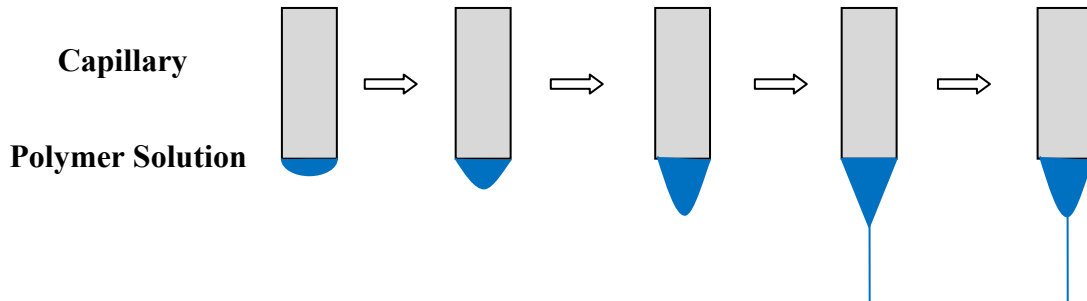
Figure 2.6 The model of polymer solution changing when electric potential increases.

2.5.2.3 Mechanisof fiber formation

In this context, mechanism of fiber formation by electrospinning was described in three steps.

a) Initiation of charged jet

The first step was subdivided into droplet generation step and a Taylor's cone formation step. The charging of a droplet of polymer solution is the initial step in electrospinning. Normally, a polymer solution is pumped at a low flow rate into a needle tip and the droplets form at end of needle is fallen off under the influence of gravity when the electric field is not too large or absence. When the droplet are charged by applying an high electric potential, the positively charged species at the needle migrate to the surface of the droplet and the negatively charged species remain inside the droplet until the electric field within the liquid droplet is zero. Charge separation will generate a force that is countered by the surface tension within the droplet.

After the polymer solution is charged, deformation of charged droplet under an electric field changed from a spherical pendant droplet to hemi spherical and then to a conical shape, which normally terms "the Taylor's cone". The solution jet is ejected from the end of Taylor's cone to collector screen, when the electrical

repulsion overcomes the surface tension. The formation of the Taylor cone is shown in Figure 2.7.

a) stage 1	b) stage 2	c) stage 3
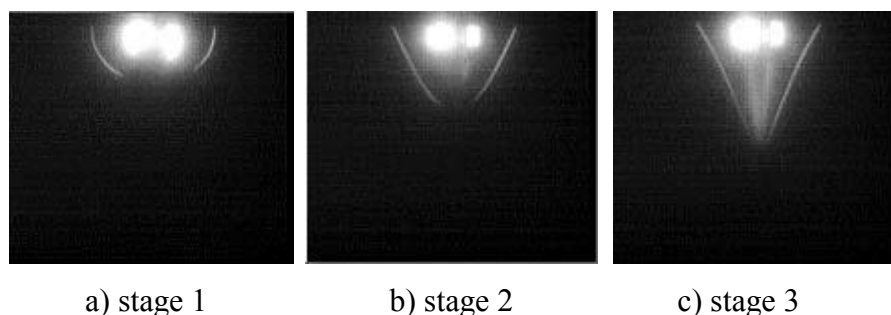
Figure 2.7 Formation of the Taylor cone. Electric potential increases with each stage until equilibrium between surface tension and the electrical force is achieved in stage 3. Image reproduced from [41]

b) Elongation of charged jet

The elongation of charged jet is continuous and random occurred while the solution jet is spouting from needle to collection screen. The columbic repulsion of surface charges on the jet has an axial component that elongates the jet in its passage towards the collector. The velocity of jet line will change, when distance is increased from Taylor's cone, the causes diameter of jet decreases rapidly length increases both extension and evaporation of the solvent. The jet reveals the variance velocity (whipping jet) when distance away from Taylor's cone, due to electrically driven bending instability of charged jet. The mode of instability obtained is dependent on the electric field, with stronger fields favoring whipping instability. The jet in this region exhibits components of electrical repulsion that are predominantly axial, thus, whipping jet is occurred.

c) Solidification of the charged jet

The Solidification of charged jet during elongation is controlled by the rate of evaporation of the solvent. The solvent evaporation can be occur before and after the charged jet collected on collection screen, which occur at increasing rates on a mass basis as the jet area dramatically increase during elongation.

For mechanism of fiber formation, the elongation of charged jet is the main parameter that influence on fiber diameter. The taper of the jet is also affected by solvent evaporation, since loss of the solvent can have a large effect on the viscoelasticity of the liquid polymer. However, other parameter such as type of polymer, processing parameters also effect on the diameter and morphology of fiber.

2.5.2.4 Parameters of electrospinning process

A proper choice of processing parameters that affect on the morphology and properties of electrospun fibers. There are many parameters that will influence the morphology of the resultant electrospun fibers. Two classes of variables that affect electrospinning can be identified from the literature: the material variables relating to polymer and solvent characteristics and the process variables concerning to either the choice of equipment or the operating parameters. For convenient of description those are classified as shown in Figure 2.8.

a) Influence of solution factor

Solution factor consist of viscosity, conductivity, surface tension, molecular weight of polymer and solvent system. The fiber diameter increases while the viscosity of solution and molecular weight of polymer increases. The fiber diameter decreases while the conductivity and temperature of solution increases. However, the trend of diameter fiber by effecting of solution factor is flexible, when some factor changes, it may affect to other factors.

b) Influence of electrospinning operating factor [42].

Electrospinning operating factor consist of applied voltage, gap distance, size of needle tip, flow rate, and polarity of tip. The fiber diameter increases by increasing of flow rate and diameter of needle. The fiber diameter decreases while the applied voltage and gab distance increases. However, the effects of applied voltage, the flow rate, diameter of the needle and the distance between the needle and the collection screen need to be considered together.

A polymer solution
- Concentration
- Solvent

Environment

Collector
- Geometry
- Dielectric properties

Material parameters

Applied potential

Feed rate

Tip of needle

Distance between needle and collector

Process parameters

Metering Pump

Syringe (Polymer solution)

Taylor Cone
Stability Region
Instability Region
Nanofibers

Target/Collection plate

High Voltage Power Supply

V

+

Figure 2.8 The basic materials and process variables in electrospinning of polymer nano fibers [40]**.**

The electrospinning process and resulting of polymer diameter or morphology is influenced by a large number of factors. So, for easy to understand those are clarify as shown in Figure 2.9

At constant electric potential, flow rate & concentration

Fiber dia.

Screen distance, cm

At constant flow rate, screen distance & concentration

Fiber dia.

Electric potential, kV

At constant electric potential, screen distance & concentration

Fiber dia.

Flow rate, ml/h

At constant electric potential, screen distance & flow rate

Fiber dia.

Concentration, wt %
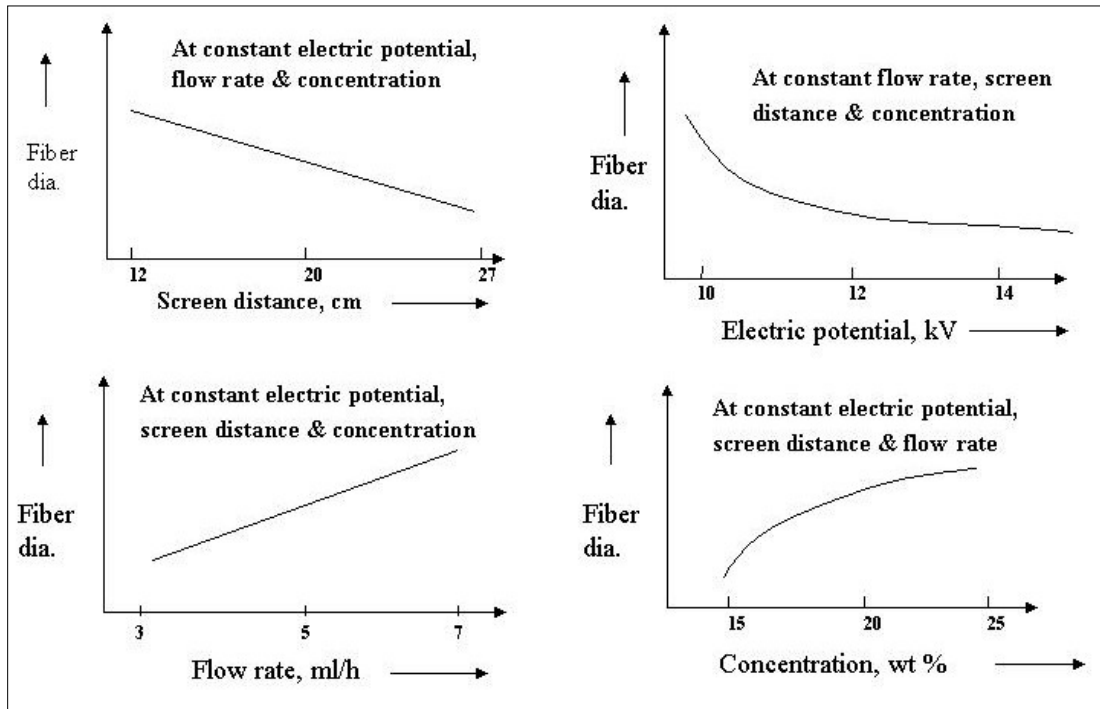
Figure 2.9 Summarizes the effects of the different parameters. **[43]**

Table 2.2 Optical sensor for heavy metals

Analyte	Reagent, transducer system	Working range or limit of detection (LOD)	Method for immobilization support material; arrangements	Other remarks	Reference
Hg(II), Cu(II)	1,10-dibenzyl-1,10-diaza-18-crown-6 and 1-(2-pyridylazo)-2-naphthol	1.0×10^{-8} M for Hg(II) and 3.2×10^{-7} M for Cu(II)	reagents are dissolved in plasticizer PVC bulk membrane	Absorbance; used PAN as a chromoionophore	[11]
Pb(II)	Gallocynine	1×10^{-1} to 1×10^{3} ppm	gallocynine is physically adsorbed on XAD-7; optical fibre chemical sensor	Loaded XAD-7 beads into the flow cell; reflectance measured; flow mode	[44]
Cu(II)	Thioxanthone derivative, 1-hydroxy-3,4-dimethylthioxanthone	1.6×10^{-7} and 1.3×10^{-2} M	reagents are dissolved in plasticizer PVC bulk membrane	Absorbance; Cu(II) forms a complex with HL and increases its absorption at 480 nm	[7]
Hg(II)	4-hydroxy salophen	1.0×10^{-6} and 1.0×10^{-2} M	Dye is covalently bonded to a triacetylcellulose film.	Absorbance; color changes from white-yellow to orange (323–429 nm)	[45]
Fe((III)	N-(4-dimethylaminophenyl)-3,5-di-t-butyl salicylaldimine (DBS)	-	fluorescent Schiff Base are dissolved in plasticizer PVC	Fluorescence; dye response to Fe(II) by decreasing the fluorescence intensity.	[46]
Co(II)	pyrogallol red	1.7×10^{-6} M up to 1.5×10^{-4} M,	Dye is covalently bonded to a cellulose acetate film	Absorbance; complex of pyrogallol red with Co(II) at 550 nm.	[47]

Table 2.2 Optical sensor for heavy metals (Cont)

Analyte	Reagent, transducer system	Working range or limit of detection (LOD)	Method for immobilization support material; arrangements	Other remarks	Reference
Cu(II)	4-decyloxy-2-(2-pyridylazo)-1-naphtanol (DPAN)	$4.5 \times 10\text{-}5$ M	DPAN is protonated and trapped inside nafion membrane; flow through optical fiber	Absorbance; Cu(II) form blue complex with DPAN	[48]
Pb(II)	2-hydroxy-1-naphthaldehydene-8-aminoquinoline (HNAAQ)	1.9×10^{-7} to 1.9×10^{-4} M	Entrapment of HNAAQ in porous gel-glasses; fluorescence probe	Fluorescence; coplanar effect and degree of molecular conjugation (Pb- HNAAQ) related fluorescence intensity	[49]
Cu(II)	2-hydroxy-1-(2-hydroxy-5-methylphenylazo)-4-naphthalenesulfonic acid (calmagite)	0.4–200 ppb	calmagite immobilized on a transparent agarose film; membrane sensor	Absorbance; changed λmax from 520to 274 nm	[50]
Hg(ll) and Cd(ll),	monofunctionalized porphyrin derivative (5-(4'-aminophenyl)-10,15,20-tris(4'-sulfonatophenyl) porphyrin, ATPPS)	1×10^{-7} M for Hg(II) and 6×10^{-7} M for Cd(II)	Receptor dye iscovalently bound to poly(2-hydroxyethylmethacrylate) (PolyHEMA); thin film chomosensor	Absorbance; Sorer bands of immobilized ATPPS at 420 nm decrease while the complex bands at 451 nm	[51]

Table 2.3 Optical sensor for nickel ion

Analyte	Reagent, transducer system	Working range or limit of detection (LOD)	Method for immobilization support material; arrangements	Other remarks	Reference
Ni(II)	3-hydroxy-3-phenyl-1-o-carboxyphenyltriazene	-	Optical solution;	Fluorescent complex formed	[52]
Ni(II)	2-(5-bromo-2-pyridylazo)-5-(diethylamino)phenol	0.5–20 ppm	Immobilized Br-PADAP into Nafion by dissolving Br-PADAP in Nafion solution; bulk and flow-through systems.	Absorbance; changing color of complex from orange to pink color with two absorption maxima at 520 and 558 nm.	[13]
Ni(II)	Thionine	1.00×10^{-10} to 1.00×10^{-7} M	Immobilized by covalent bornding of thionine in agarose membrane; placed optode membrane inside the quartz cell.	Absorbance; complex is formed at 610 nm.	[53]
Ni(II)	2-amino-1-cyclopentene-1-dithiocarboxylic acid (ACDA)	5.0×10^{-6} to 1.0×10^{-3} M	Immobilized reagent by binding ACDA to a cellulose acetate film; optical chemical sensor (optode) placed inside the quartz cell.	Absorbance; Ni(II)-ACDA in membrane is 535 nm	[15]
Ni(II)	Dimethyglyoxime (DMG)	1.8-5.0 ppm	Multiplexed colorimetric solid-phase extraction	Diffuse reflectance 550 nm	[11]
Ni(II)	Dimethyglyoxime (DMG)	0.5-5.0 ppm	Colorimetric solid-phase extraction	Diffuse reflectance 550 nm	[28]
Ni(II)	Dimethyglyoxime (DMG)	10-200 ppm	Impregnation; red complex	Reflectance test strip of Merck	[54]

CHAPTER III

EXPERIMENTAL

3.1 Apparatus

The apparatuses used in this study are listed in Table 3.2.

Table 3.1 Apparatus lists

Apparatus	Company, model	Purpose
1. Fourier transform infrared spectrometer (FT-IR)	Perkin Elmer, model Spectrum one. Attenuated Total Reflectance (ATR) mode	Identification of functional groups of sensors
2. Thermogravimetric analyzer (TGA)	Perkin-Elmer: Pyris 1	Confirmation the forming of Ni(DMG)$_2$complex
3. Inductively coupled plasma-atomic emission spectroscopy (ICP-OES)	Thermo sciencetific, iCAP 6000 series	Metal ion determination (operating parameters are shown in table 3.2)
4. Scanning electron microscope (SEM)	JEDL, model JSM-5410LV Japan	Morphology characterization
5. UV-visible spectrophotometer	Hewlett Packard 8453	Record spectra and absorbance measurements
6. Fibre-optic spectrophotometer	Ocean optic redpide USB 650	Record spectra and reflectance measurements
7. Conductivity/TDS/0C/F meter	Butech instruments, model CON 510	Conductivity measurements

Apparatus	Model (company)	Purpose
8. Programmable Viscosity	Brookfiled, model DV-II	Viscosity measurements
9. High voltage supply	Spellman CZE 1000R	Electrospinning set-up
10. Syringe pump	QIS, model NE1000	Electrospinning set-up
11. pH meter	Metron, Model 744 pH meter	pH measurement

Table 3.2 Operating parameters the determination of nickelconcentration by ICP-OES

Operating conditions	Nickel
Wavelength (nm)	221.6
Sample introduction	Nebulizer
Sample flush time (s)	30.0
Pump stabilization time (s)	5.0
Nebulizer gas flo$w$ (L/min)	0.50
Auxilliry gas flow (L/min)	0.50
Flus pump rate (rpm)	50
RF power (W)	1150
Analy pump rate (rpm)	50
Coolant gas flow (L/min)	12.00

3.2 Chemicals

All chemicals used for sensor preparation were purchased in analytical grade form suppliers listed in Table 3.3.

Table 3.3 Chemicals list

Chemicals	Supplier
High molecular weight (mw 80,000) Polycarpolactone, PCL	Sigma Aldrich
Gelatin	Sigma Aldrich
Dimethyglyoxime, DMG	Merck
Dichlorometane,DCM	Carlo Erba
N, N-dimethyformamide, DMF	Merck
Tetrahydrofuran, THF	Merck
Actone	Merck
25% Ammonia solution	Merck
Nitric acid, HNO_3	Merck
Standard heavy metal solution	Merck
Ni standard solution (1000 mg L^{-1})	BDH SpectrosoL
Pb standard solution (1000 mg L^{-1})	BDH SpectrosoL
Cd standard solution (1000 mg L^{-1})	BDH SpectrosoL
Co standard solution (1000 mg L^{-1})	BDH SpectrosoL
Cu standard solution (1000 mg L^{-1})	BDH SpectrosoL
Mn standard solution (1000 mg L^{-1})	BDH SpectrosoL
Fe standard solution (1000 mg L^{-1})	BDH SpectrosoL
Na standard solution (1000 mg L^{-1})	BDH SpectrosoL

3.2.1 Preparation of Reagents

a) DMG solution

1.5% (w/v) of DMG solution was prepared by dissolving 1.5 g of gelatin in ethanol and the solution was stirred under ambient temperature for 1 h.

b) Nickel standard solutions

Nickel standard solutions were prepared by dilution of 1000 mg L^{-1} stock standard solution to the desired concentrations with DI water. The pH value was adjusted using ammonia solution and nitric acid solutions.

c) Nitric acid solution

Nitric acid solutions (1, 5 and 10 % v/v) for pH adjustment were prepared daily by direct dilution of the concentrated solution (65%).

d) Ammonium solutions

Ammonium solution solutions (1, 5 and 10 % v/v) for pH adjustment were prepared daily by direct dilution of the concentrated solution (25%).

e) Solution containing different metal ions

The solutions of different metal ions Cd^{2+}, Co^{2+}, Cu^{2+}, Mn^{3+}, Fe^{2+}, Pb^{+} or Na^{+}, used in the study of effect of interference ions on sensor performance were prepared by dilution of 1000 mg L^{-1} stock standard solution with DI water to the required concentrations.

f) Nickel working standard solutions

Nickel working standard solutions was prepared by dilution of 1000 mg L^{-1} nickel standard solution to the required concentrations with DI water. The working standard solutions were prepared freshly before used.

3.3 Sensor fabrication

3.3.1. Fabrication of PCL electrospun fibers doped with DMG

The 16% PCL solution was prepared by dissolving PCL 1.6 g in 10 mL studied solvents such as acetone, THF and mixed solvent of DCM/DMF (50/50). Then, DMG powder was added in PCL solution to achieve mass ratio of 10:90, 20:80 and 30:70. The solutions were kept under stirring condition for 6 h. The polymer solutions were placed in 10 mL plastic syringe with a needle tip of 0.6 mm in diameter. Electrospinning process was carried out under the varied electric fields of 10, 15 and 20 kV and varied distances between the needle tip and the collector of 10, 15 and 20 cm. The feeding rate of the solution was controlled at 1.2 mL/h. The electrospun fibers were collected on aluminum foil covered on the rotator surface. All experiments were carried out at room temperature.

A basic apparatus of electrospinning process include of high voltage supply (Spellman CZE 1000R), syringe pump (QIS, model NE1000) and rotated collector was set-up for electrospinning process. The experiment setup is depicted in Figure.3.1
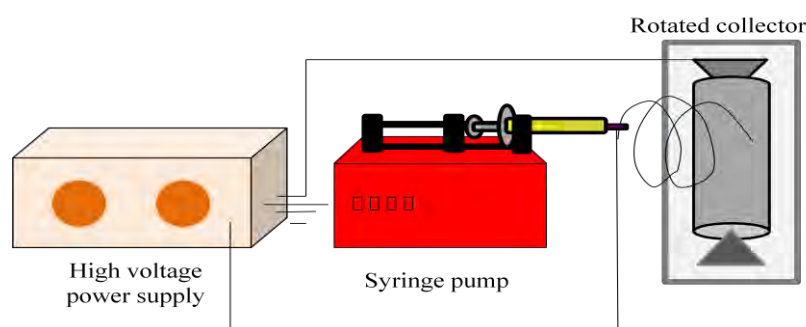
Figure 3.1 Schematic of the electrospinning process.

3.3.2 Fabrication of PCL doped DMG film casting

The 5 % PCL solution was prepared by dissolving 0.5 g of PCL in 10 mL of studied solvents such as acetone, THF and DCM/DCM (50/50 v/v). In case of acetone, a warm water bath (40 ^{0}C) was used. Then, DMG was added in PCL solution to achieve the mass ratio of 10:90, 20:80 and 30:70. The mixtures were stirred for 6 h.

The solution was poured on the glass Petri dish (diameter 9.0 cm), which was covered with a lid (diameter 10.0 cm) and placed in fume hood at room temperature for the slow evaporate [36]. The resulting films were further dried for 24 h. at ambient temperature in a desiccator to remove the residual organic solvent and moisture.

3.3.3 Fabrication of gelatin doped DMG film castings

A 10% (w/v) of gelatin solutions was prepared by dissolving 10 g of gelatin in DI water and the solution was stirred under temperature at 90 $^{\circ}$C for 2 h. Then, the DMG in ethanol solution was added in gelatin solutions to the required amount of DMG and the mixture was stirred for 1 h. Gelatins containing different mass of DMG were prepared by mixing the gelatin solution and different concentration of DMG in ethanol solution as described in Table 3.1. The fleshly solutions were prepared for film casting. The solution was casted on the plastic Petri dish. The resulting films were further dried for 24 h at ambient temperature. For the crosslinking, films were kept in vacuum oven under temperature of 140 ^{0}C for 48 h (Dehydrothermal treatment, DHT) [55] and kept in desiccators before use.

Table 3.4 The amount of components in gelatin doped DMG film casting sensor

Polymer solution	GEL		DMG		GEL : DMG
	% wt/v	mL	% wt/v	mL	% wt
1. GEL-DMG; A	10	8	0.175	8	98.3 : 1.7
2. GEL-DMG; B	10	8	0.375	8	96.4 : 3.6
3. GEL-DMG; C	10	8	0.750	8	93.0 : 6.0
4. GEL-DMG; D	10	8	1.125	8	89.9 : 10.1
5. GEL-DMG; E	10	8	1.50	8	87.0 : 13.0

3.4 Characterization

3.4.1 Scanning Electron Microscope (SEM)

Surface morphology all of these types of sensor were characterized using scanning electron microscope (SEM). The diameter of fibers was reported as the average values with standard deviation (n=50) by SemAfore program.

3.4.2 Fourier Transform Infrared Spectrometer (FTIR)

ATR-FTIR was used to identify the characteristic functional groups of polymer blaned with DMG. Infrared spectra were recorded by Attenuated Total Reflectance (ATR) mode using a FT-IR spectrometer in the wavenumber range of 400 - 4000 cm^{-1} using the absorbance mode with 32 scans.

3.4.3. Thermal Gravimetric Analysis (TGA)

Thermogravimetric measurements were performed using a heating rate of 20 ºC min^{-1} for temperation range of 200-900 ^{0}C under nitrogen atmosphere. TGA was used to confirm the formation of Ni(DMG)$_2$ complex.

3.5 Sensor performance testing

a) PCL/DMG sensor

The 3X3 cm^2 PCL sensors were cut and placed in nickel (II) solutions for 10 minutes. The color change was observed by visual detection parallel with the reflectance spectrophotometer. The reflectance measurement was obtained from died PCL senor, after dipped in nickel (II) solutions; sensor was kept at ambient condition for drying. All reflectance spectra were measured with fiber-optic spectrophotometer (Ocean optic red tide USB 650). The reflectance was measured under dark condition by using back box to minimize any interference from ambient light. The reflectance measurement set-up was shown in Figure 3.2. The calibration curve of reflectance signal was plotted in term of Kubelka-Munk function. The Kubelka-Munk function, *F(R)*, is define as: $F(R) = (1-R)^2/2R$, where *R* is the percent reflectance with respect to

the standard white. *F(R)* can be related to analyte concentration by $F(R) = 2.303\varepsilon C/s$, where ε is absorbtivity, C the concentration of the $Ni(DMG)_2$, and s the scattering coefficient of sample surface. The reflectance was recorded at 547 and 550 nm of PCL/DMG fiber and PCL/DMG film casting sensor, respectively.
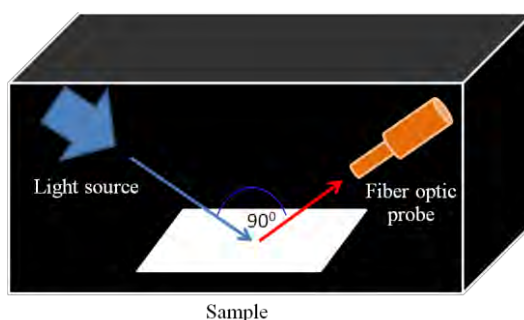
Figure 3.2 Schematic of the reflectance measurement homemade setup.

b) Gelatin/DMG sensor

The 1X3 cm^2 gelatin/DMG sensors were cut and placed in films holder, polystyrene cuvettes pathlength 1.0 cm. Then, 3 mL of Ni (II) solution was added in cuvette for 10 minute. After that, the transmission spectra of gelatin films sensor testing were collected at 550 nm. The reflectance signal was detected from gelatin/DMG films and solution; light source pass through both of film and solution.

3.5.1 Effect of solution pH

The effect of pH on sensor responsding was studied in the range of pH 4.0 to 11.0 which contained 5ppm of nickel (II) ion. The adjustment of pH was done with ammonium solution (1, 5 and 10 % v/v) or nitric acid solutions (1, 5 and 10 % v/v). The experiments were performed in triplicate.

3.5.2 Response time

The response time of purpose method were studied by varying the dipping time of sensor in 5ppm of nickel solutions at pH 9. The times of 5, 10, 20, 30 and 60 minutes were used in this study.

3.5.3 Effect of interference ions

The effects of several interfering ions to $Ni(DMG)_2$ complex were examined by adding the other coexisting ions such as Cd(II), Co(II), Cu(II), Mn(II), Pb(II) Fe(III) and Na(I) in the concentration of 5 and 50 mgL^{-1} to nickel solutions (5 ppm). This experiment was carried under optimum condition; nickel solution pH 9.0 and response time at 10 minute.

3.6 Method validation

Validation of purpose method was the measurement of performance characteristic such as accuracy, precision, limit of detection, limit of quantitative and linear range. The reproducibility was studied in this part as well.

For the reproducibility, the sensor was tested by immersing in 5 ppm nickel solution of same stock solution at pH 9 for 10 minute. This experiment was performed by using the sensor that fabricated in different day of 10 day. This experiment was performed in 5 replicates for each sample.

The calibration curve was constructed by varying nickel concentration of 1, 2, 3, 4, 5, 8 and 10 ppm. For PCL/DMG fiber and film, sensors were immersed in nickel solution at pH 9 for 10 minute. Then, sensor was kept in room temperature for drying before reflectance measurement. For gelatin/DMG film, sensor was placed in polystyrene cuvettes and then nickel solution was added into cuvettes. The absorbance was collected from passed through signal of the both of film and solution. The method validation was performed by using spike water sample with standard nickel concentration at two concentration level (1 and 5 ppm) chosen from the concentration within the linear range of calibration curve. The linearity plotted by the nickel concentration versus the absorbance and reflectance. Each experiment was repeated 7 times at the optimum condition; nickel solution pH 9, dipping time 10 minute. The accuracy and the precision were presented as recovery (%) and the relative standard deviation (%), respectively. The detection limit and limit of quantitative were calculated from the standard deviation of 20 measurements of reagent blank using the purpose method.

3.7 Real sample analysis

The application of propose sensor to determine nickel (II) ions is real waters sample was demonstrated under the optimum conditions. The results obtained were compared with the results determined by ICP-OES (Inductively Couple Plasma Optical Emission Spectrometry)

Three of water sample (rinsing water from gold and silver line of jewelry industrial and waste water from nickel alloys industry) was collected in the polyethylene bottle and adjusted to low pH with nitric acid. All of water sample was filtered to remove particle before use. The water samples were spiked with standard nickle(II) at three concentration levels: 0.7, 1 and 5 mg L^{-1} and adjusted pH to pH 9 with ammonium solution. The nickel concentration of 0.1, 0.5, 1, 2, 3, 4, 5, 8 and 10 ppm was used to calibration curve construction. The reflectance and absorbance measurement were preformed under optimum condition; pH 9, dipping time at 10 minute. The experiment was performed in 5 replicates for each sample.

CHAPTER IV

RESULTS AND DISCUSSION

In this study, the colorimetric sensors to determine nickel ions concentration were developed by using dimethyl glyoxime (DMG) as complexing reagent. Two polymer types including polycarbonlactone (PCL) as hydrophobic polymer and gelatin as hydrophilic polymer were used in this study as the media. The PCL/DMG sensors were fabricated by two different processes: electrospining and casting methods. Moreover, gelatin/DMG was casted as colorimetric sensor for nickel ions as well. The sensor performance was evaluated and validated. Finally, the fabricated sensor is applies to real sample analysis.

4.1. PCL electrospun fibers doped with DMG

4.1.1. Fiber formation and morphology of electrospun PCL doped DMG mats

The morphology and diameter of electrospun fibers were depended on the various parameters, mainly electrospinning process and the polymer solution properties [40]. In this research, electric potential and distance between needle and collection screen were studied as factor of electrospinning process. The amount of DMG in polymer solution and effect of solvent type were studied as well. The SEM photographs and diameter of fibers were evaluated for optimize the condition of electrospinning of PCL doped DMG fibers. Then, the electrospun fibers were characterized by using FT-IR and TGA.

4.1.1.1. Effect of electric field and the distance between needle and collector on fibers morphology

The effects of applied electric potential on morphology and diameter of fiber need to be considered together with distance between the needle and the collection

screen because change of distance between the needle and the collection screen influences directly electric field generated by electric potential [40].

The scanning electron microscope (SEM) micrographs of the 16% PCL fibers of the variation of the electric filed and the distance between needle to collection screen were shown in Figure 4.1. Generally, the formation of bead may be expected at the time during electrospinning whenever the surface tension forces tend to overcome the force (such as charge repulsion and viscoelastic force) [40]. The formation of beads was only observed on the SEM micrographs when the PCL fiber was spun at the potential below 20 kV. It was indicated that at potential below 20 kV, the charge repulsion forces could not overcome the surface tension forces. Therefore, the fibers were spun using 20 kV in this study, while the effect of distance between needle and collector on the diameter size was found to be small. However, we chose to work at the distance of 20 cm as it produced the most uniform fibers (280$\pm$51 nm) when compared to the distance of 15 cm (290$\pm$56 nm) and 10 cm (285$\pm$76 nm).The average diameter of PCL fibers in different conditions were shown in Table 4.1.

Table 4.1 The characteristics of electrospun PCL fibers at various electric potential and the distance between needle and collection screen

Electric potential (kV)	Distances (cm)	Fiber formation	Average diameter of fiber (nm) (n=50)
10	10	Bead fibers	-
	15	Bead fibers	-
	20	Bead fibers	-
15	10	Bead fibers	350+107
	15	Bead fibers	345$\pm$91
	20	Bead fibers	331$\pm$87
20	10	fibers	285$\pm$76
	15	fibers	290$\pm$56
	20	fibers	280$\pm$51
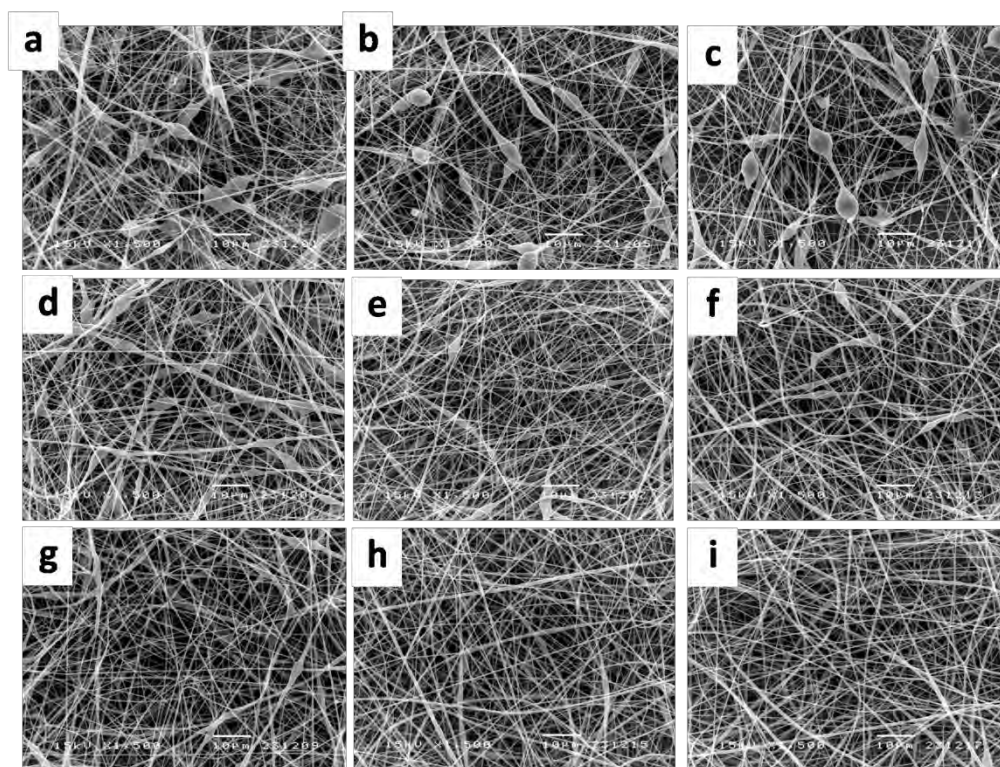
Figure 4.1 SEM micrographs of electrospun fibers of 16% PCL in DMF/DCM. a) 10 kV, 10 cm b) 10 kV, 15 cm c)10 kV, 20 cm d) 15 kV, 10 cm e) 15 kV, 15 cm f) 15kV, 20cm g) 20kV, 10cm h)20 kV, 15cm i) 20kv, 20 cm, respectively. Original magnification 1,500x. electrospinning condition.

4.1.1.2 Study of the suitable spinning condition for PCL/DMG blend fibers and the effect of mass ratio on the fiber morphology

This part, the effect of the DMG on morphology and diameter of the eletrospun fibers was studied. In figure 4.2 shown the SEM micrographs of 16% PCL/DMG blend fibers in mass ratio of 20:80 at different electrospinning conditions. The SEM observation of PCL/DMG blend fibers shown the same trends of fibers diameter and morphology with pure PCL electrospun fibers, the formation of beads was only observed when the PCL/DMG fibers was spun at the potential below 20 kV. The effect of distance between needle and collector on the diameter size was also found to be small. The diameter of fibers was reported as the average values with standard deviation in Table 4.2. It was indicated that addition of DMG had a small effect on the morphology and diameters of PCL electrospun fiber.
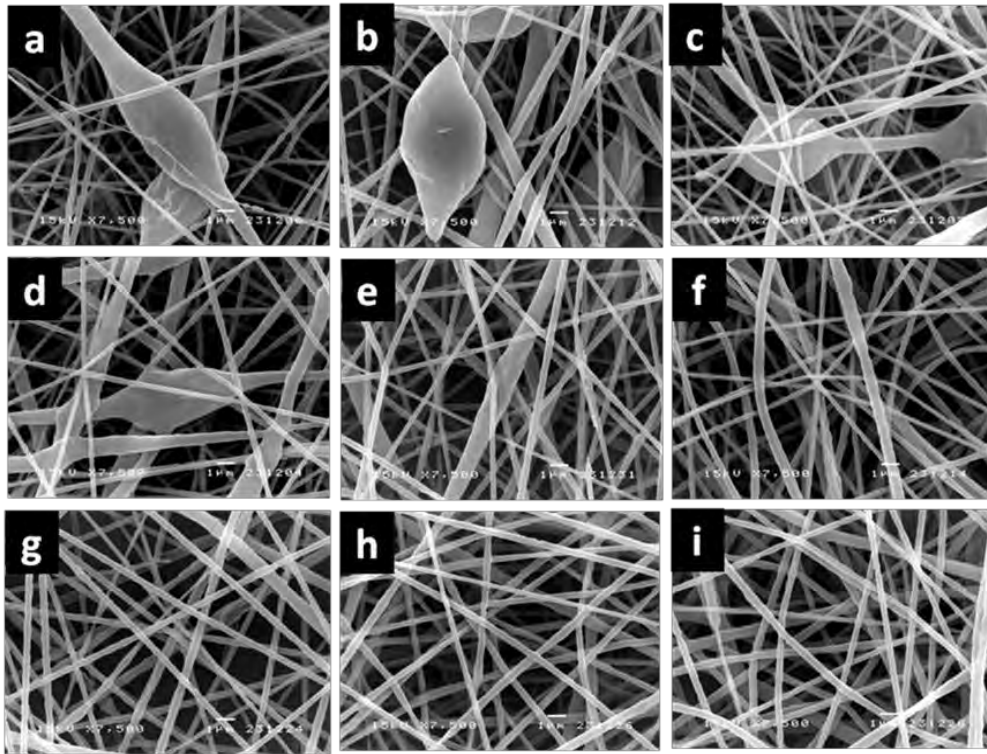
Figure 4.2 SEM micrographs of 16% PCL/DMG blend fibers in mass ratio of 20:80 at different electrospinning conditions. a) 10 kV, 10 cm b) 10 kV, 15 cm c)10 kV, 20 cm d) 15 kV, 10 cm e) 15 kV, 15 cm f) 15kV, 20cm g) 20kV, 10cm h)20 kV, 15cm i) 20kv, 20 cm. Original magnification 7,500x. electrospinning condition.

Table 4.2 The characteristics of electrospun PCL/DMG blend fibers at various electric potential and the distance between needle and collection screen.

Electric potential (kV)	Distances (cm)	Fiber formation	Average diameter of fiber (nm) (n=50)
10	10	Bead fibers	-
	15	Bead fibers	-
	20	Bead fibers	-
15	10	Bead fibers	-
	15	fibers	296±104
	20	fibers	291±79
20	10	fibers	274+58
	15	fibers	275±61
	20	fibers	275±39

The effect of different amount of DMG in PCL solution on morphology and diameters of PCL electrospun fiber was also studied in order to obtain the largest mass ratio of PCL/DMG. As shown in the SEM micrographs (Figure 4.3), the electrospun fibers of PCL containing DMG in mass ratios of 90:10, 80:20 and 70:30 were fabricated. However, electrospun fibers of the PCL/DMG having a mass ratio higher than 70:30 could not be fabricated due to the solubility limit of DMG in PCL solution. With the increasing of DMG content from 0% to 30%, the average size of fiber diameters were 280±51, 270±34, 275±39 and 273±56 nm, respectively. This suggested that the addition of DMG into the PCL solution has a minor effect on the diameter of electrospun fibers. This might be explained by the viscosity and conductivity of the PCL/DMG solutions as shown in Table 4.3. The increase in the viscosity should result in the bigger diameter fibers, whereas the fiber diameter should decrease with the increase of solution conductivity [42]. For the mixture of PCL/DMG, we observed these counterforce which resulted in the relatively diameter fibers as reported
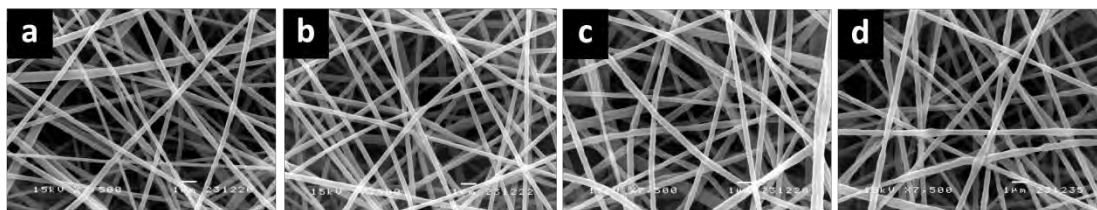
Figure 4.3 SEM micrographs of 16% PCL/DMG blend fibers in different weight ratio [DMG:PCL]. a) pure PCL, b) 10:90, c) 20:80 and d) 30:70. Original magnification 7,500x.

Table 4.3 The changing polymer solution properties when DMG was added into the PCL solution.

Sample	Viscosity (cp, centipoint)	Conductivity (µs)
Pure 16%PCl	1401	0.12
16%PCl [90:10]PCL:DMG	1794	0.53
16%PCl [80:20]PCL:DMG	1909	0.79
16%PCl [70:30]PCL:DMG	2024	0.85

4.1.1.3 Effect of solvent type on electrospun fibers morphology

The variation of solvents such as acetone and THF was studied to compare with DCM/DMF. The SEM images of PCL in different solvent type electrospun fibers were shown in Figure 4.4. From the SEM observations, the electrospun fiber produced from the PCL solution of acetone and THF showed the bead on string mophology, whereas those from the solutions of DCM/DMF did not. By refering to the pysical data of solvent used (in Table 4.4), the electrospun fibers diameters observed was found to decrease with an increase in the boilding point of the solvents. The electrospun diameters of PCL in acetone (1140± 870 nm) and THF (560±240 nm) showed the large fibers diameter more than PCL in DCM/DMF (280±60 nm)

electrospun fibers. The smaller fibers diameter result from jet extension because DCM/DMF has a high boiling temperature so the jet will have more time for the solvent to be evaporated. The hiher volatility does not allow enough time coarening of the fibers, the jet clould not be streached much further.

The variation of solvents such as acetone and THF was studied to compare with DCM/DMF. The SEM images of PCL electrospun fibers in different solvent types were shown in Figure 4.4. The PCL electrospun fiber diameters using acetone and THF as solvents are 1140± 870 nm and560±240 nm,respectively. Under the same spinning condition, these spun fibers were larger than the PCL spun fibers using DCM/DMF as solvents (280±60 nm).Moreover, in comparison with DCM/DMF (50/50), the bead formation on electrospun fibers were only found when using the acetone and THF as solvents. This trend might be caused by the diffrences in boiling points where the higer volatility (lower boiling point) does not allow enough time coarening of the fibers, the jet clould not be streached much further reulted in the bead formation in acetoen and THF (Table 4.4).

| Average 1140± 870 nm | Average 560±240 nm | Average 280±60 nm |
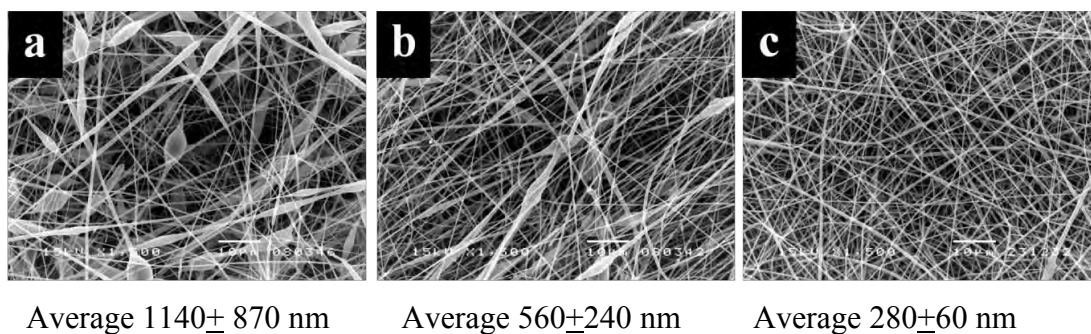
Figure 4.4 SEM micrographs of 16% PCL fibers in different Solvent. a) acetone, b) THF and c) DMF/DCM. Original magnification 1,500x. electrospinning condition.

Table 4.4 Properties of solvents used in this work **[65]**

Solvent	Boiling point (^{0}C)	Density (g/cm^3)	Solubility parameter (MPa)$^{1/2}$	Dipole moment (Debye)	Dielectric constant
Acetone	56.3	0.786	19.7	2.70	20.7
Tetrahydrofuran (THF)	65.5	0.885	18.5	1.75	7.47
Dichlorometane (DCM)	83.5	1.239	20.2	1.86	8.93
Dimethyformamide (DMF)	153.0	0.940	24.0	3.82	37.06

4.1.14 Characterization of PCL electrospun fibers doped with DMG

The FT-IR spectra of PCL, DMG, and PCL doped with DMG fibers were shown in Figure 4.5. The peaks located at 2945 and 2865 cm^{-1} of PCL fibers (Figure 4.5 (a)) were assigned as the stretching vibrations of -CH$_2$-, while the peak at 1727 [56] and 1185 [57]cm^{-1} were assigned as vibration of –C=O and stretching vibrations of -C-O, respectively. In the case of DMG (Figure 4.5 (b)), the broad peak at 3205 cm^{-1} is attributed to the stretching vibrations –O-H. The weak peak at 2930 cm^{-1} is due to the stretching vibrations of –C-H and the sharp peak at 979 is due to vibration of –N-O- [58]. There were no differences in the peak positions, were noted between DMG and PCL doped with DMG spectra (Figure 4.5 (b) and (c)). This may be explained as the molecular interaction between PCL and DMG were weak. These two components were simply blended. Figure 4.5 (d) showed the spectrum of the immersed PCL containing DMG fibers in nickel solution. The peak of 3205 cm^{-1} of DMG was not observed. It should be due to the strong hydrogen bonding resulting in the shift of –O-H stretching mode to a lower frequency [59]. The addition peak at 1572 cm^{-1} could be attributed to the –C=N stretching mode in the Ni(DMG)$_2$

complex, whereas it does not appear in the DMG or PCL/DMG spectrum. The appearance of the unique peak (v_{CN} stretching) in Figure 4.5 (d) was <u>established</u> that Ni(DMG)$_2$ complexes were formed.
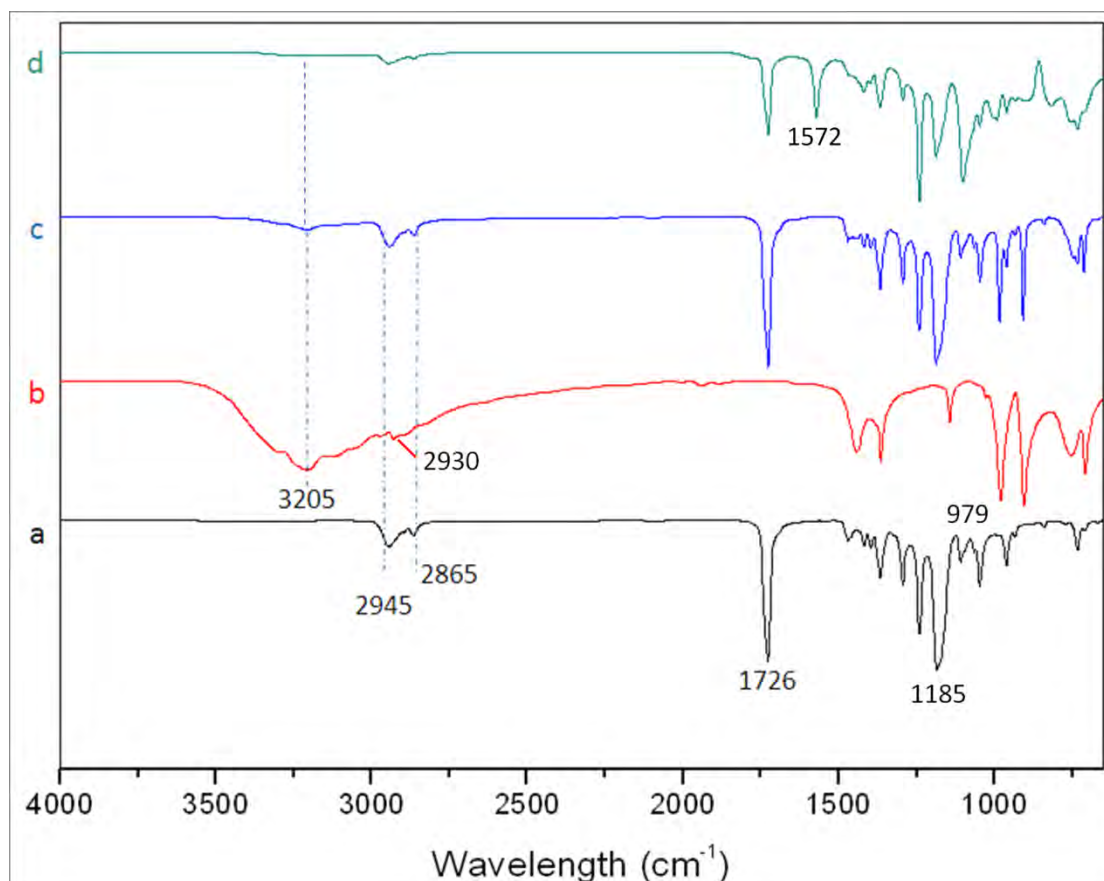
Figure 4.5 FTIR spectra. a) 16%PCL electrospun fibers, b) DMG, c) PCL/DMG blend fibers and d) PCL/DMG blend fibers immersed in nickel (II) solution. Two wavelengths (3205 and 1572 cm^{-1}) of interest were indicated for the comparison purpose

Figure 4.6 shows the thermogravimetric analysis (TGA) themogram of electrospun PCL fibers in Figure 4.6 (a), NI(DMG)$_2$ complex in Figure 4.6 (b), electrospun PCL fibers containing DMG in Figure 4.6 (c) and electrospun PCL fibers containing DMG immersed in 10 ppm nickel solution in Figure 4.6 (d). The different mass loss between PCL/DMG and PCL/Ni(DMG)$_2$ (Figure 4.6 (c) and (d)) were found. It was implied that Ni(DMG)$_2$ were formed.
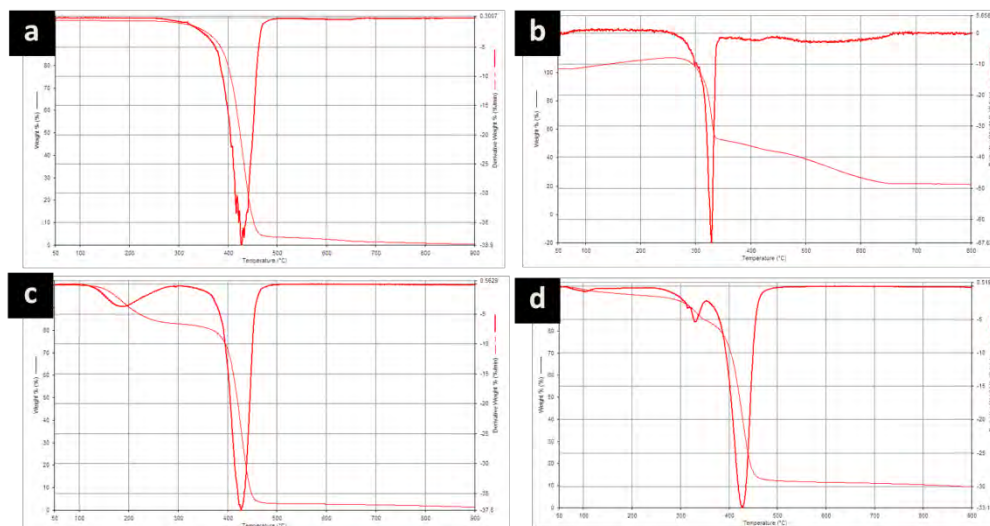
Figure 4.6 Thermogravimetric analysis (TGA) curve of a) electrospun PCL fibers, b) NI(DMG)$_2$ complex, c) electrospun PCL fibers containing DMG d) electrospun PCL fibers containing DMG immersed in 10 ppm nickel solution.

4.1.2 Sensor performance testing

4.1.2.1 Effect of pH on performance of sensor

Nickel is usually present in the +2 oxidation state, which forms a 1:2 stoichiometric complex with DMG [27]. Moreover, the complexation of nickel with DMG involves the loss of proton, so the rate and extent of complexation are pH dependent. The effect of pH on the complexation efficiencies of Ni(DMG)$_2$ was investigated in the pH range of 5-11. The results were depicted in Figure 4.7. The complexation efficiencies of Ni(DMG)$_2$ increased as the pH of nickel solution increased from 5 to 9, then it reduced with further increase in pH. It may be explained by the precipitation of Ni(OH)$_2$ at pH 10 and 11. From Figure 4.7, the suitable pH for complexation of nickel with DMG is at pH 8 and 9. However, at pH 9 the better reproducibility was obtained. Therefore, pH 9 were chosen in all further experiments.
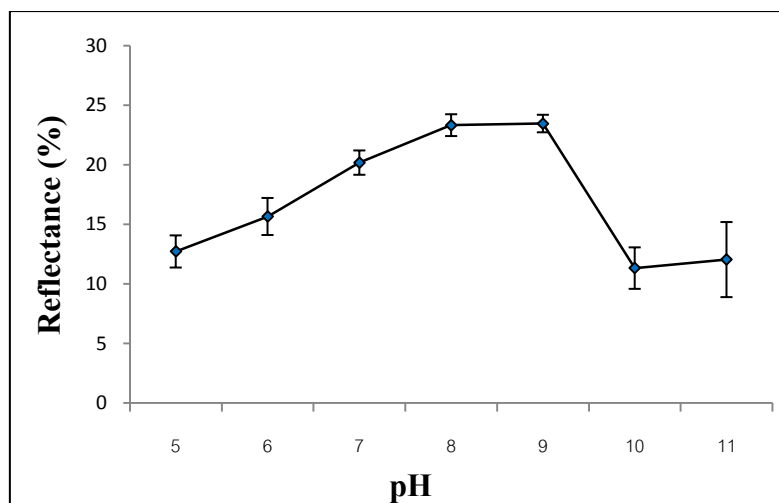
Figure 4.7 Effect of pH on the complexation of Ni(DMG)$_2$ of PCL electrospun fibers doped with DMG sensor

4.1.2.2 Effect of DMG quantity on performance of sensor

The effect of DMG quantity on sensor performance was investigated by measuring reflectance signal using fiber optic spectrophotometer. The reflectance signal of this experiment was shown in Figure 4.8. It was seen that the sensitivity was increased with an increase in the amount of DMG. Although, the amount of Ni(DMG)$_2$ complexes were formed more with the sensor with mass ratio of 30:70 (DMG: PCL), the sensor with the mass ratio of 20:80 was selected for nickel detection in this work due to the better precision results.
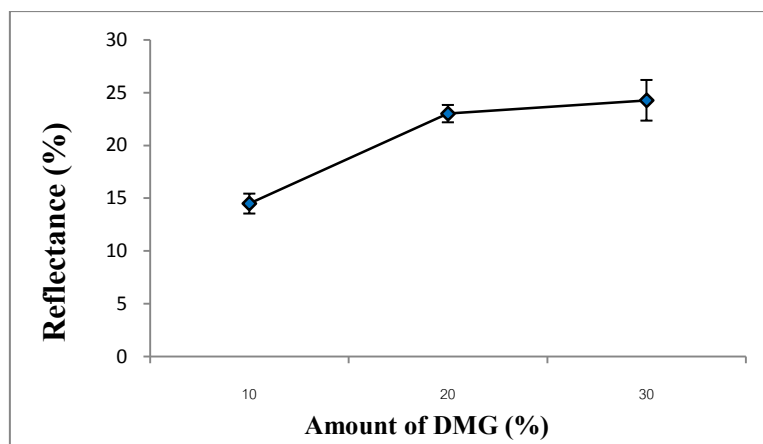
Figure 4.8 Effect of DMG quantity on PCL electrospun fibers doped with DMG sensor sensor performance

4.1.2.3 Response time

One of the important parameters of optical sensor is response time. The response time of sensor was controlled by the time required for complexation between nickel and DMG. The reflectance of $Ni(DMG)_2$ on sensor was recorded at 550 nm over the period time of 60 minute. The response increased from 1 to 10 minutes and then leveled off, indicating that 10 minute dipping time is the suitable for the analysis. Therefore, 10 minute of dipping time was used in all further experiments.
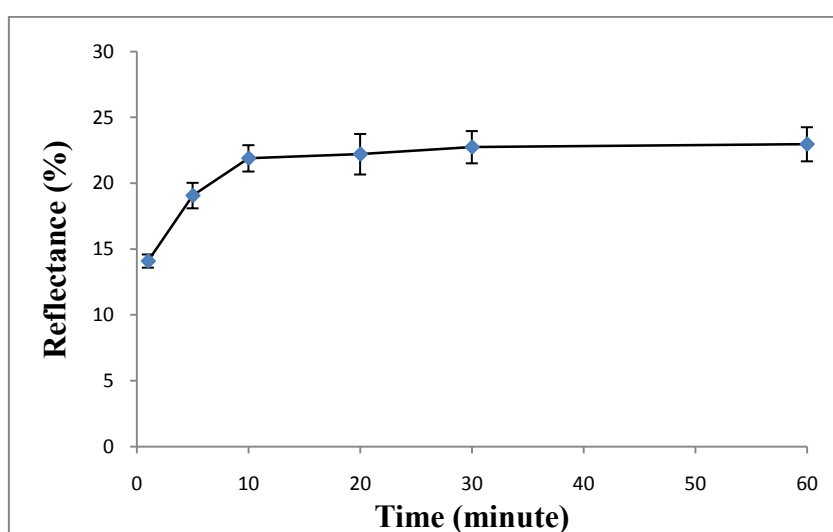
Figure 4.9 Response times of PCL electrospun fibers doped with DMG sensor sensor in present of 5ppm nickel solution.

4.1.2.4 Effect of interference ions

There are several interfering species to the $Ni(DMG)_2$ complex. Iron(III), manganese(II) and copper(II) [60] have all been shown to interfere with the complexation of nickel with DMG [28]. To determine the extent of interference from each species, individual solutions containing 5 ppm of cadmium(II), cobalt(II), copper(II), iron(III), manganese(II), lead(II) and sodium were prepared by diluting of standard solution 1000 ppm of those species. These ions are target analytes for waste water regulation [2] and are likely to co-exist with nickel (II). When dipped PCL/DMG electrospun fiber sensor into pure ions interference of 5 ppm concentration. All of the species tested, not produced signals at 550 nm that could interrupt for signal of $Ni(DMG)_2$. Solutions containing equal concentrations (5 ppm) and a 10-fold (50 ppm) of interference were analyzed. The results of interference studies are summarized in Table 4.5. Cadmium(II), copper(II), manganese(II) and sodium, did not interfere when present at similar concentrations to nickel. However, a 10-fold of interference, these studied interference ions with at least 10 times more concentrated than nickel (II) could interfere the response of the proposed sensor except cadmium(II), manganese(II) and sodium. For this experiment, sodium ions not interfered to nickel ions may be due to sodium could not form complex with DMG.

Table 4.5 Interference studies using 1:1 and 10:1 ratios of interferant of nickel of PCL electrospun fibers doped with DMG sensor

Ni 5 ppm	Interference	1 fold (5ppm)	10 fold (50ppm)
	Cd	4.8±0.1	4.3±0.2
	Cu	4.7±0.1	1.5±0.3
	Co	2.9±0.2	2.3±0.1
4.9±0.1	Fe	1.2±0.3	0.5±0.2
	Mn	4.9±0.2	4.6±0.1
	Na	4.8±0.2	4.5±0.1
	pb	2.6±0.2	2.0±2.0

4.2 PCL doped with DMG film castings

4.2.1. Film formation and morphology of PCL doped with DMG film castings

4.2.1.1 Effect of DMG amount on films surface morphology

The composition of DMG and PCL in mass ratio including 10:90, 20:80 and 30:70 were studied to explore the suitable preparing condition for nickel detection. Our goal was to fabricate a nice uniformly distributed colorimetric reagent film. From the consideration in Figure 4.10, there were no any formations of crystalline rods on the surface of PCL/DMG films with the mass ratio of 90:10and 80:20 comparing to PCL/DMG films with the mass ratio of 70:30 (Fig. 4.10 (c)). It was implied that the excess DMG might be formed on films surface, which is not suitable for this study. The average pore sizes of PCL/DMG films were declined with increasing amount of DMG in PCL solution. The average pore diameter of PCL/DMG films in 10:90 and 20:80 of mass ratio were 10.15$\pm$2.44 and 6.48$\pm$2.04 μm, respectively. Therefore, we chose to prepare Ni (II) sensor using 80:20 mass ratio.
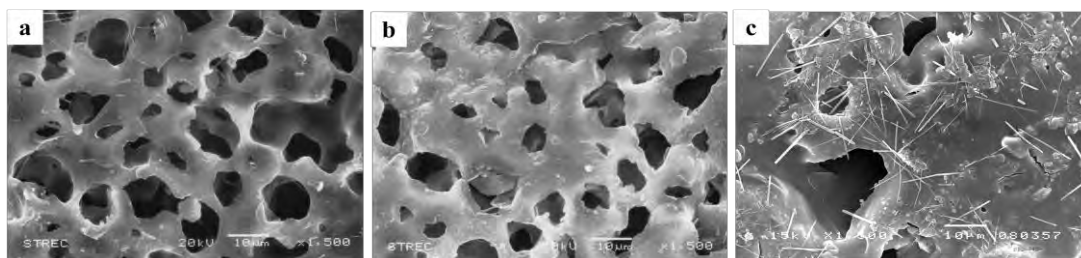
Figure 4.10 Effect of DMG quantity on the surface morphology of solution cast PCL/DMG films (a) 10:90 [DMG:PCL], (b) 20:80 [DMG:PCL] and (c) 30:70 [DMG:PCL]. The scale bar shown in each micrograph is 100 μm in length (x1500 magnification

4.2.1.2 Effect of solvent type on films surface morphology

In Figure. 4.11 shown the surface morphology of the casting PCL/DMG films prepared in three different solvents. The casting PCL/DMG films prepared in all solvents was porous (Figure 4.11 (a) and (b)). PCL films cast using acetone exhibited

more porous comparing to flims preapring with THF and DCM/DMF. This might be due to the evaporation rate of acetone is higher than the other solvents. Moreover, the PCL/DMG films using acetone and THF as solvents were distorted, whereas there was no any film distortion prepared by using DCM/DMF as solvent. Even though, the porosities of casting film prepared in acetone and THF were higher compare to the one prepared in DCM/DMF solvent, the distorted films were not suitable for using as naked-eye sensors, (Figure 4.11 (c)). Therefore, the DCM/DMF was chosen as the working solvent for casting PCL/DMG films in subsequent experiments
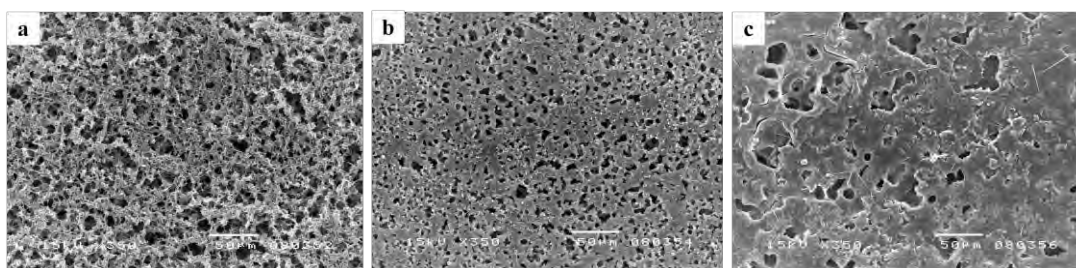
Figure 4.11 Effect of solvent on the surface morphology of casting PCL/DMG films in the mass ratio of 80:20 using different solvents; a) acetone b) THF and c) DCM/DMF. The scale bar shown in each micrograph is 50 μm in length (x350 magnification)

4.2.1.3 Characterization of PCL films doped with DMG

The comparison of FT-IR spectrum between PCL/DMG preparing by casting and electrospining processes was shown in Figure 4.12. The spectrum of both sensors were similar this due to the similarity of chemical structure of film and fibres. The discussion of PCL doped with DMG had been explained in content of 4.1.1.4.
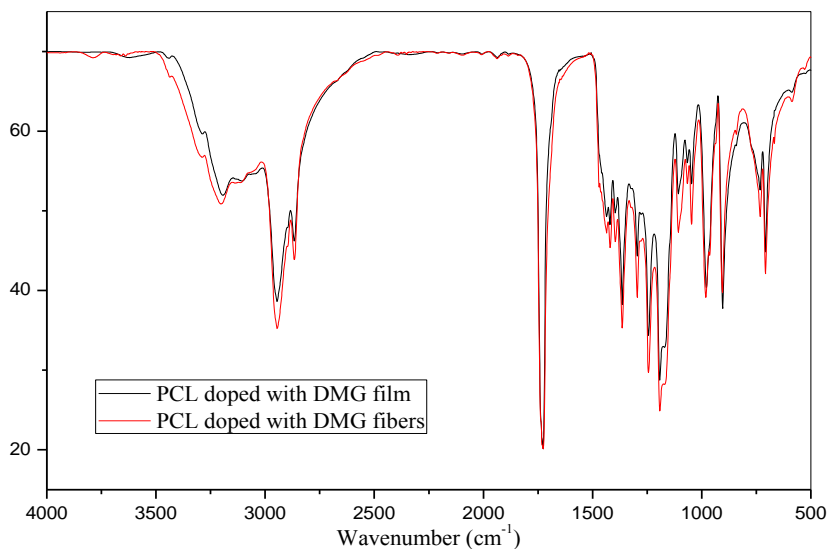
Figure 4.12 FTIR spectra of PCL/DMG films and fibres

In Figure 4.13 shows the spectra of PCL doped with DMG films and PCL doped with DMG films immersed in nickel (II) solution. The result show addition peak at 1572 cm^{-1} could be attributed to the $-C=N$ stretching mode in the Ni(DMG)$_2$ similar to PCL doped with DMG electrospun fibres.
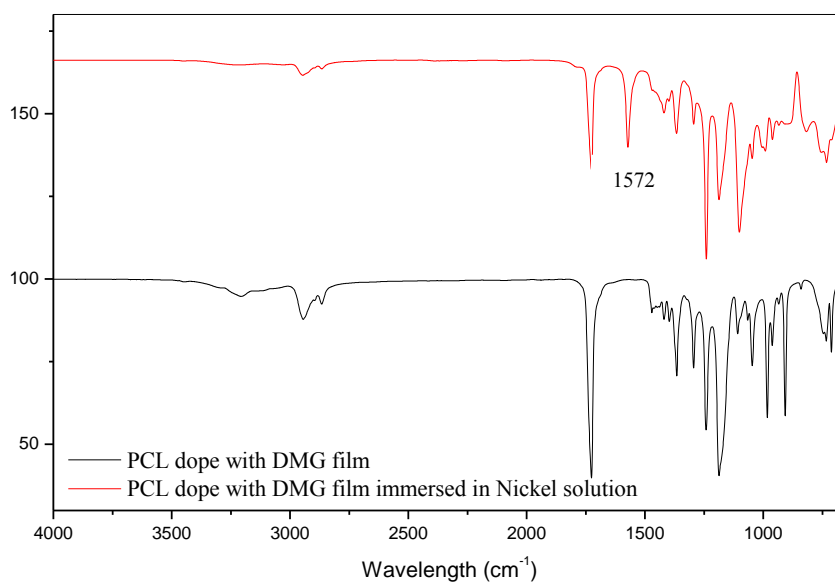
Figure 4.13 FTIR spectra PCL doped with DMG film and PCL doped with DMG film immersed in nickel (II) solution.

4.2.2 Sensor performance testing

4.2.2.1 Effect of pH on performance of sensor

The influences of pH on the performance of PCL/DMG film casting as sensor were investigated in pH range of 5-11. The results presented in Figure 4.14. In similarity with PCL/DMG blend spun fibers, pH 8 and 9 were found to be the suitable pH for nickel (II) analysis. However, the trend of reflectance intensity of PCL/DMG film casting was higher than PCL/DMG electrospun fiber this is due to the larger content of DMG in a sensor.
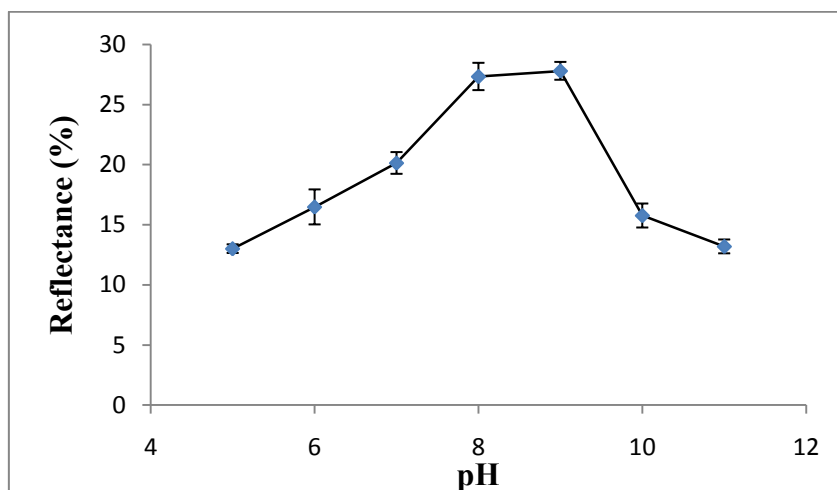
Figure 4.14 Effect of pH on the sensor efficiencies of PCL/DMG film casting

4.2.2.2 Effect of DMG quantity on performance of sensor

The analytical signal of this experiment was shown in Figure 4.15. It was seen that the response was increased with an increase in the amount of DMG similar to PCL/DMG electrospun fiber performance. In this part, the mass ratio 20:80 was selected as well.
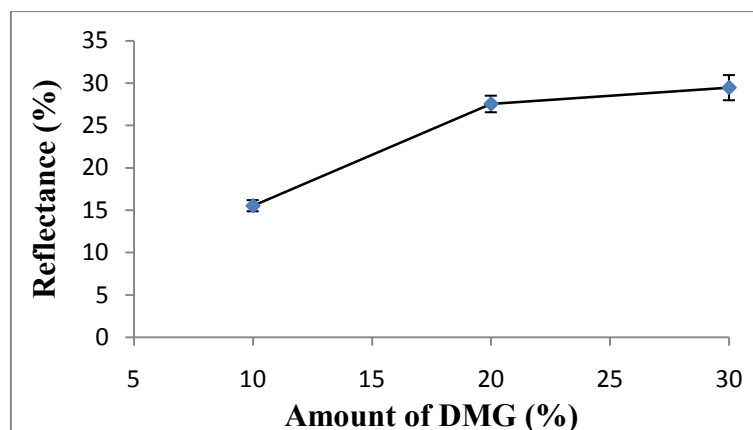
Figure 4.15 Effect of DMG quantity on the sensor performance of PCL/DMG films.

4.2.2.3 Response time

The reflectance of $Ni(DMG)_2$ on sensor was recorded by fiber optics spectrophotometer at 547 nm over the period time of 60 minute. Figure 4.16 shows the response time of sensor. Similar trend between PCL/DMG film cast and electrospun fiber was observed that the reflectance signal increased from 1 to 10 minutes, then it remained constant with further increased in times. Therefore, the 10 minute of dipping time is suitable for both sensors: PCL doped with DMG electrospun fiber and PCL doped with DMG film cast.
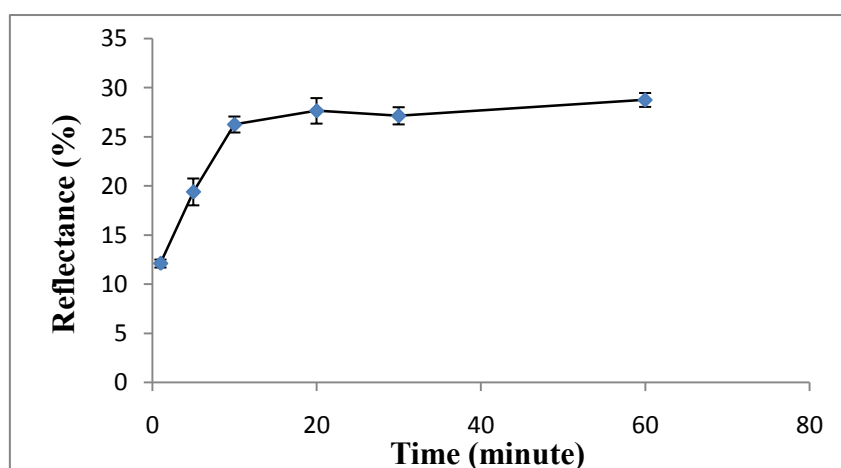
Figure 4.16 Response time of PCL/DMG film cast in present of 5ppm nickel solution at pH 9.

4.2.2.4 Effect of interference ions

In this section, we studied the interferences of several anions and cations that are abundant in water samples and have influence on the performance of this sensor. The species of interference in this part had been discussed in content 4.2.2.4. The result of interference studies were summarized in Table 4.6. Cadmium(II), copper(II), manganese(II) and sodium showed no any interference to determination nickel when presented at an equal concentrations. All species except manganese could interfere with the nickel detection when the concentration of interference was 10times larger than nickel (II) concentration. The similar result was observed in the PCL/DMG electrospun fiber study as well due to similarity of chemical structure of film and fiber.

Table 4.6 Interference studies using 1:1 and 10:1 ratios of interferant of nickel PCL doped with DMG film casting sensor

Ni 5 ppm	Interference	1 fold (5ppm)	10 fold (50ppm)
	Cd	4.8 ± 0.1	4.5 ± 0.2
	Cu	5.1 ± 0.2	2.1 ± 0.2
	Co	2.7 ± 0.2	1.7 ± 0.4
5.0 ± 0.2	Fe	2.5 ± 0.3	0.4 ± 0.3
	Mn	5.0 ± 0.1	5.0 ± 0.2
	Na	5.0 ± 0.2	4.6 ± 0.2
	pb	1.7 ± 0.3	1.6 ± 0.1

4.3 Gelatin doped with DMG film casting

Gelatin, a hydrophilic polymer, can be dissolved in warm water and fabricated in various form. For comparison with PCL, which is hydrophobic, gelatin was used as the media for developing nickel sensor in this study.

4.3.1 Characterization of gelatin doped with DMG film casting

According to gelatin is hydrophilic polymer that can dissolve in water. So, the crosslinking of gelatin film was studied. In this part, the gelatin doped with DMG was characterized in 2 forms:crosslinked and non-crosslinked gelatin films. Gelatin film casting was crosslinked by dehydrothermal treatment (DHT) at 140 ∘C for 48 h. The FT-IR spectra of gelatin were shown in Figure 4.17. The peaks located at 3450 cm^{-1} and 3420 cm^{-1} were assigned as the –N-H stretching of secondary amide [61], while the peaks located at 1650 and 1550 cm^{-1} were assigned as amide carbonyl –C=O stretching and –N-H in plane blending, respectively [62]. After crosslinking, dehydrothermal treatment can generate chemical bounding between the carboxylic and amino groups in gelatin. So, the crosslinked gelatin by using DHT can occur only when the amino and carboxylic groups are close to each other [63]. The degree of crosslink reacation can be observed by analysis the amide peak at 1550 cm^{-1}. The peak located at 1550 cm^{-1} is proportional to the amount of NH$_2$ which is changed to NH during the formation of the crosslink bonds. For this reason, a decrease in intensity of peak at 1550 cm^{-1} corresponds to an increase the number of crosslink [64]. The spectra of gelatin doped with DMG films before and after crosslinking were shown in Figure 4.17. The results showed the same spectra between gelatin/DMG film casting before and after crosslinking. However, it was postulated that the crosslink may be formed because the gelatin/DMG film casting after crosslink by DTH did not dissolve in water.
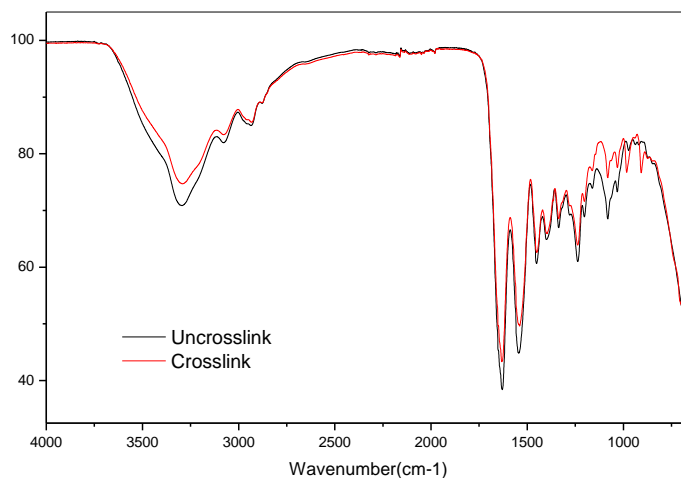
Figure 4.17 FTIR spectra of gelatin doped with DMG films before and after crosslinking.
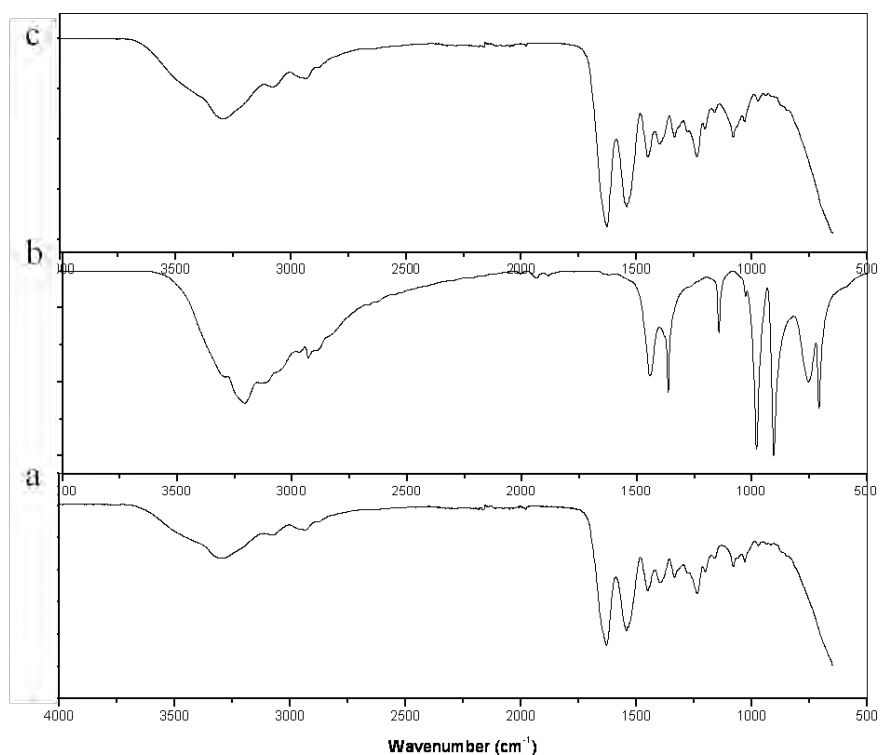
Figure 4.18 FTIR spectra of a) gelatin film casting, b) DMG and c) gelatine/DMG film casting.

Figure 4.18 shown FT-IR spectra of crosslinked gelatine film, DMG and gelatine/DMGfilm. From this result, the spectra of gelatine film was similar to and

gelatine/DMG film. This might imply that there is no interaction forming between gelatine and DMG molecules.

The spectrum between gelatine/DMG film and gelatine/DMG film after immersed in nickel solution were compared in figure 4.19. Normally, the –C=N stretching mode of Ni(DMG)$_2$ should be observed at 1572 cm^{-1}, where could not be seen in this study. It might be overlapped by the large –N-H stretching peak at 1550 cm^{-1}of gelatin and C=N stretching mode in Ni(DMG)$_2$ at 1572 peak. Therefore, it is hard to observe the change in FI-IR spectra of gelatine/DMG film after immersed in nickel solution.
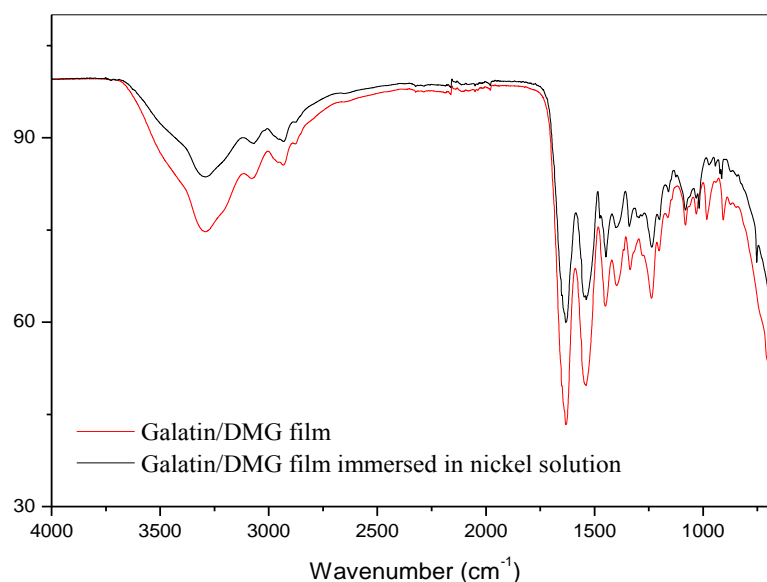
Figure 4.19 FTIR spectra of gelatine/DMG film and gelatine/DMG film after immersed in nickel solution.

4.3.2 Sensor performance testing

4.3.2.1 Effect of pH on performance of sensor

The influences of pH on the performance of Gelatin/DMG film as sensor were investigated in pH range of 5-11. The pH of nickel solutions was prepared in content 3.2.1. The results were presented in Figure 4.20. The maximum response was obtained at pH 9. At pH above 9, the reduced response is due to the precipitation of

nickel hydroxide (K_{sp}.of $Ni(OH)_2$ = 2.0×10^{-15}). So, pH 9 solutions were use in all further experiments
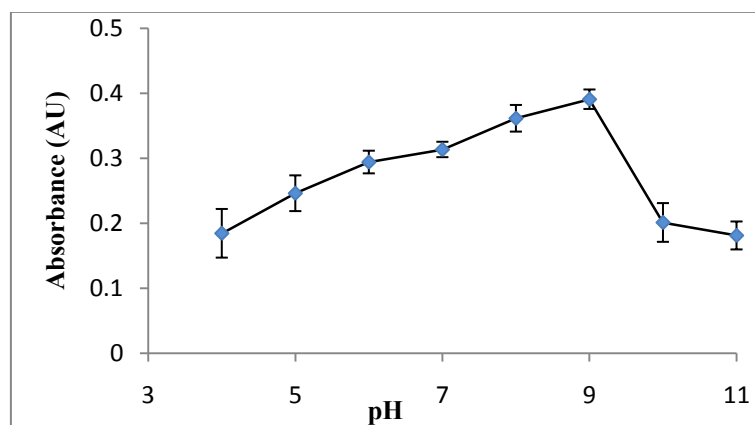
Figure 4.20 Effect of pH on the sensor efficiencies of PCL/DMG film.

4.3.2.2 Effect of DMG quantity on performance of sensor

Gelatins containing different of DMG solutions were described in Table 3.4. The 1x3 cm^2 gelatin/DMG films with various mass ratios were prepared as shown in Table 4.7.

Table 4.7 The amount of gelatin and DMG in 1x3 cm^2 of film casting

Polymer solution	GEL	DMG	GEL : DMG
	mg	mg	% wt/wt
1. A	40	0.7	98.3 : 1.7
2. B	40	1.5	96.4 : 3.6
3. C	40	3.0	93.0 : 6.0
4. D	40	4.5	89.9 : 10.1
5. E	40	6.0	87.0 : 13.0

The effect of DMG quantity on physical appearance and sensor performance by using UV-Visible spectrophotometer was investigated. From Figure 4.21, the transparent gelatin films were transformed to translucent films when DMG was added

in gelatin. The analytical signal of this experiment was shown in Figure 4.22. It was seen that the response increased with an increase in the amount of DMG. However, the sensors C, D and E which contained more amount of DMG, produced a larger standard deviation. This might be due to the forming of DMG precipitates in the film creating the heterogeneous film. In this work, the amount of DMG of 1.5 mg was selected for nickel detection because it delivered the good absorbance intensity with a small standard deviation.
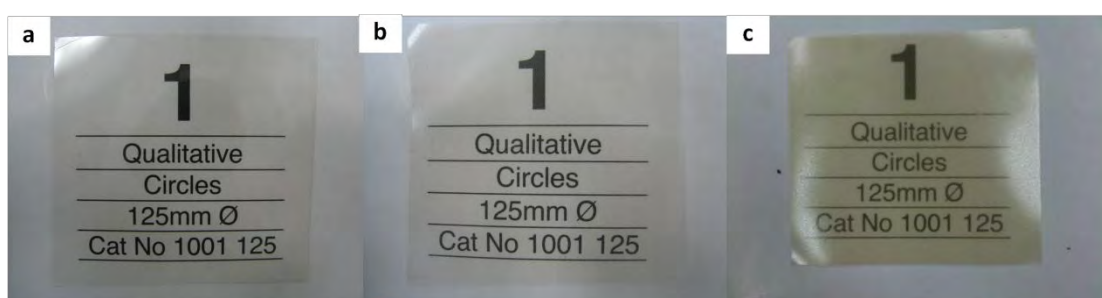
Figure 4.21 Image gelatin film in different amount of DMG a) Pure gelatin film, b) gelatin/DMG [96.4:3.6] (sensor B) and c) gelatin/DMG [87.0:13.0] (sensor c).
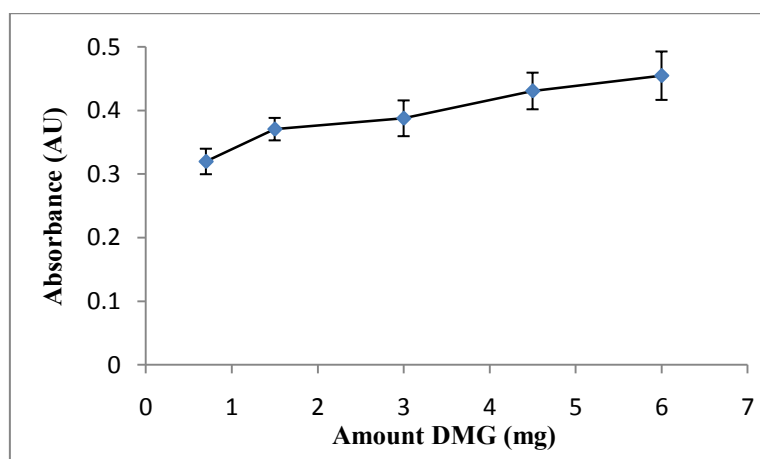
Figure 4.22 Effect of DMG quantity on the performance of PCL/DMG film sensor

4.3.2.3 Response time

The response time of this sensor was investigated by using 1, 5 and 10 ppm of nickel solution at pH 9. The absorbance of Ni $(DMG)_2$ on sensor was recorded by UV-visible spectrophotometer at 550 nm over the period time of 60 minute. The

responses time of sensor were shown in Figure 4.23. For every concentration, the similar trend was seen where the absorbance increased with time until 10 minutes. Then, the response was relatively constant. Therefore, 10 minute of dipping time was chosen to use in further experiments as well.
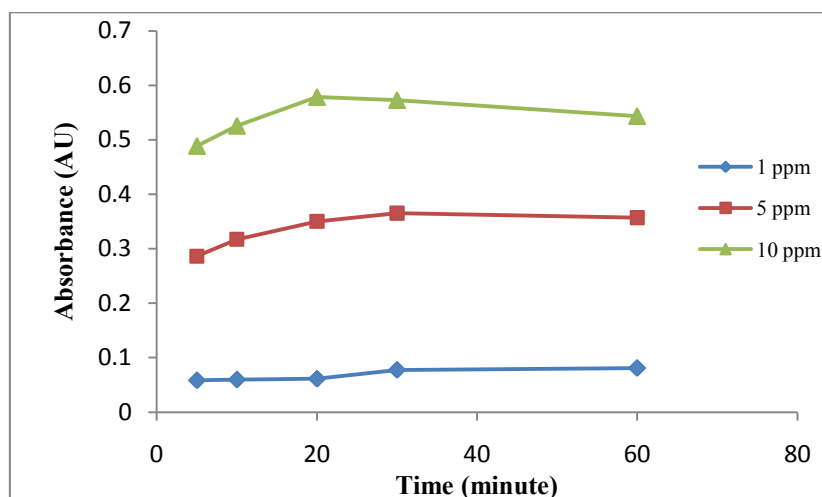
Figure 4.23 Response time of gelatin/DMG film (mass ratio of 80:20) sensor in presence of 1, 5 and 10 ppm nickel solutions (pH 9).

4.1.3.6 Effect of interference ions

The species of interference in this part had been discussed in content 4.1.2.4. The result of interference studies are summarized in Table 4.8. At the same concentration level, the manganese and sodium ions showed small interference with the nickel detection. However, the presences of other interfering ions caused a negative deviation in the nickel analysis. In the case of the interference concentration 10 times higher than nickel concentration, all species except sodium ions interfered with the nickel detection. This result might be due to the competition between these ions and nickel ions with DMG forming complex.

Table 4.8 Interference studies using 1:1 and 10:1 ratios of interferant of nickel of Gelatin doped with DMG film casting sensor

Ni 5 ppm	Interference	1 fold (5ppm)	10 fold (50ppm)
	Cd	4.0±0.6	3.0±0.4
	Co	3.5±0.3	2.0±0.4
	Cu	2.1±0.6	0.8±0.3
4.8±0.3	Fe	1.8±0.4	1.7±0.6
	Mn	4.2±0.6	2.3±0.4
	Na	4.7±0.4	4.3±0.4
	pb	3.7±0.5	2.3±0.5

4.4 Sensor efficiency and method validation

4.4.1 The visual detection and response spectra of sensor

4.4.1.1 PCL electrospun fibers doped with DMG

Complexation between nickel (II) ions and DMG formed a red-pink complex on the electrospun mats, which we could observe by naked-eye in concentration range of 1-10 ppm as shown in Figure 4.24. The sensor was immersed in various concentration of nickel (II) solution at pH 9 for 10 minutes, which is the optimum condition. The complex formation was also investigated by using spectrophotometer, which was confirmed that PCL electrospun fibers containing DMG can be used for detecting nickel (II) ions. The reflectance spectra of $NI(DMG)_2$ were shown in Figure 4.25. The maximum wavelength of $Ni(DMG)2$ complex was observed at 550 nm.
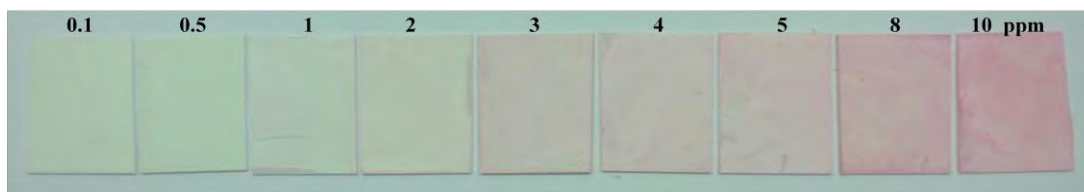
Figure 4.24 Sensor images of PCL/DMG electrospun fibers that immersed in nickel solutions at concentration of 0.1, 0.5, 1, 2, 3, 4, 5, 8 and 10 ppm for 10 minute.
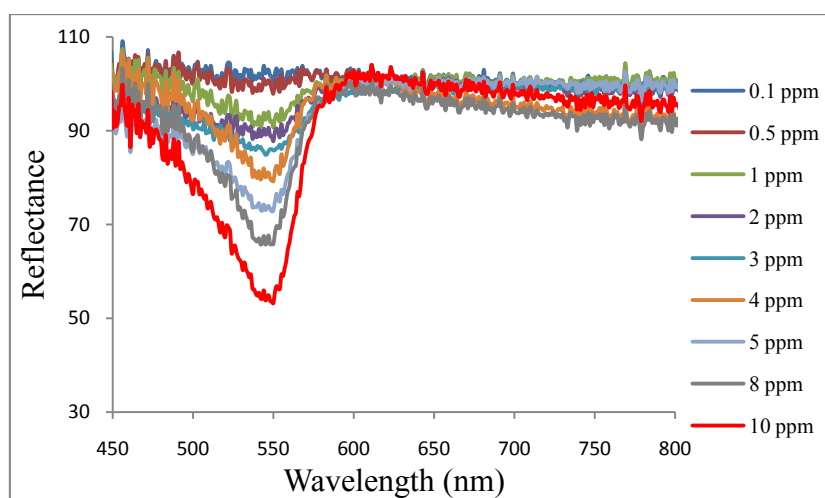
Figure 4.25 The reflectance spectra of PCL/DMG electrospun fibers that immersed in nickel solutions at concentration of 0.1, 0.5, 1, 2, 3, 4, 5, 8 and 10 ppm.

Because the surface of spun fiber sensor is not smooth that could produce diffuse reflection, therefore, the Kubelka-Munk function ($F(R)_{547}$) was used to construct the calibration curve instead of the reflectance values. The calibration curve for determination of nickel ions in the range of 1-10 ppm using PCL/DMG electrospun fibers was shown in Figure 4.26(b). From this result, it can be said that the response of sensor depended linearity on the nickel concentration between 1and 10 ppm with $F(R) = 2.0282x + 1.1375$ and $R^2 = 0.9925$.
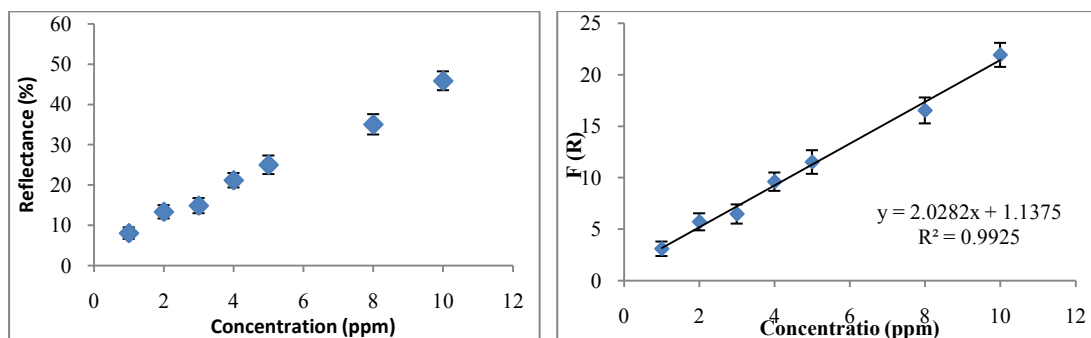
Figure 4.26 (a) The reflectance responding and (b) calibration curve for determination of nickel ions using the optimum conditions for the range 1-10 ppm of PCL/DMG electrospun fibers

4.4.1.2 PCL doped with DMG film casting

The visual detection of $Ni(DMG)_2$, a red-pink complex on the film surface, was shown in Figure 4.27. The result was very encouraging. The complex of nickel (II) ions and DMG could be observed by naked-eye.The reflectance response was evaluated using fiber optic spectrophotometer shown in Figure 2.8. From the spectra, the wavelength at 547 nm was used as the detection wavelength for further study.
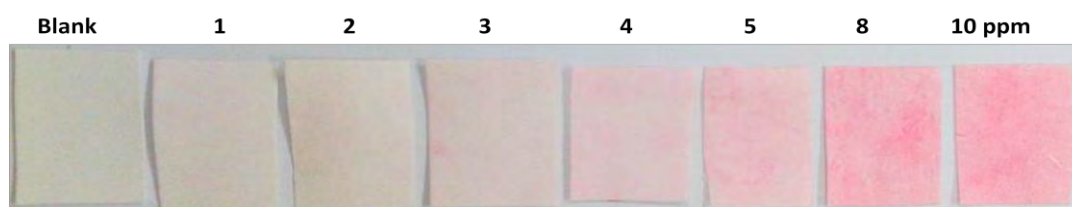
Figure 4.27 Sensor images of PCL/DMG film casting that immersed in nickel solutions at concentration of 1, 2, 3, 4, 5, 8 and 10 ppm for 10 minute.
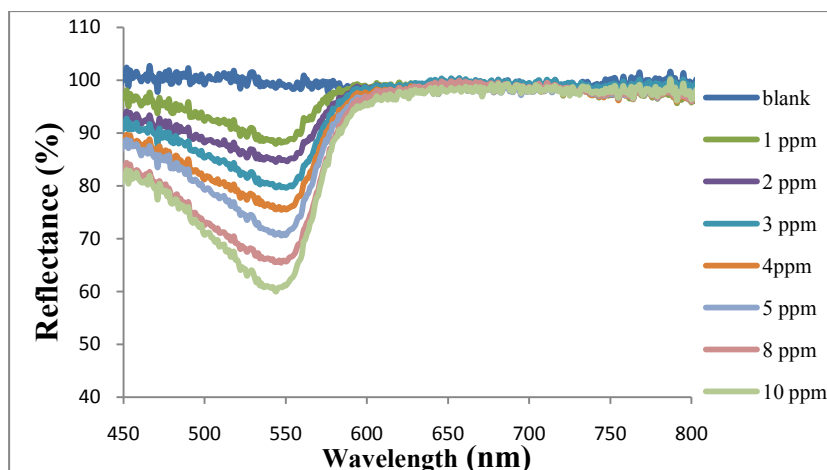
Figure 4.28 The reflectance spectra of PCL/DMG film that immersed in nickel solution at concentration of 1, 2, 3, 4, 5, 8 and 10 ppm.

The reflectance response and the calibration curve of this sensor was shown in Figure 4.29. The equation from the Kubelka-Munk (F(R) plot was obtained; F(R) =2.0515x+27919 and R^2= 0.9964.
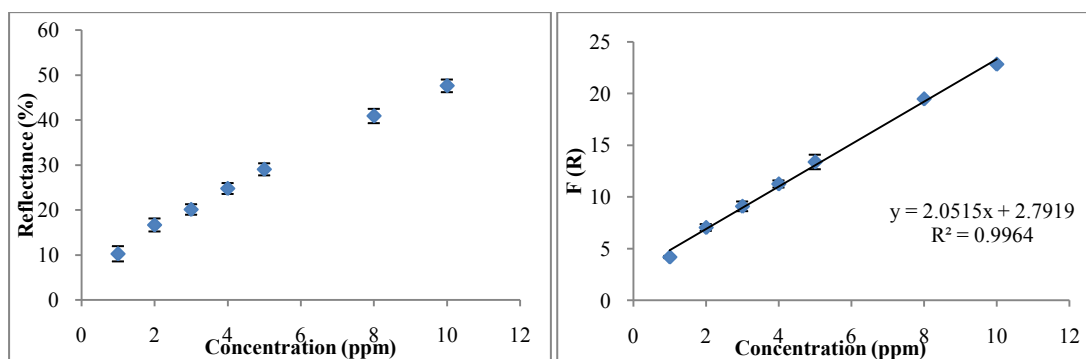
Figure 4.29 (a) The reflectance response and (b) F(R) calibration curve of the PCL/DMG films using the obtained optimum conditions for sensing nickel with concentration of 1 to 10 ppm.

4.4.1.3 Gelatin doped with DMG film casting

Figure 4.30 shown the visual detection of Ni(DMG)$_2$ complex on gelatin/DMG film when immersed in nickel solution in range of 1 to 10 ppm at pH 9 for 10 minutes. The complex formation was also investigated by using UV-visible

spectrophotometer and shown in Figure 4.31. The maximum wavelength of Ni(DMG)$_2$ complex was observed at 550 nm.
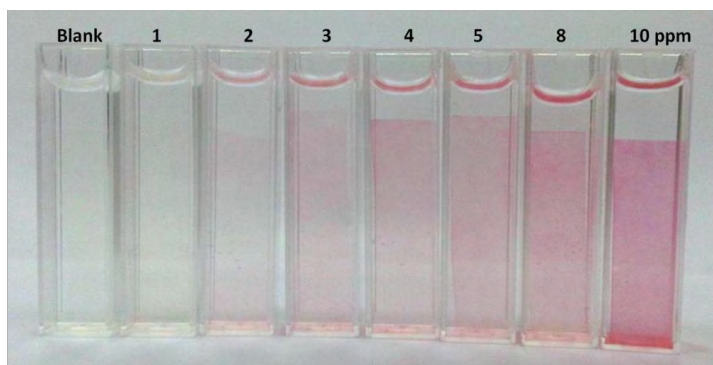
Figure 4.30 Sensor images of gelatin/DMG film cast that immersed in pH 9 nickel solutions with concentration of 1, 2, 3, 4, 5, 8 and 10 ppm for 10 minute.
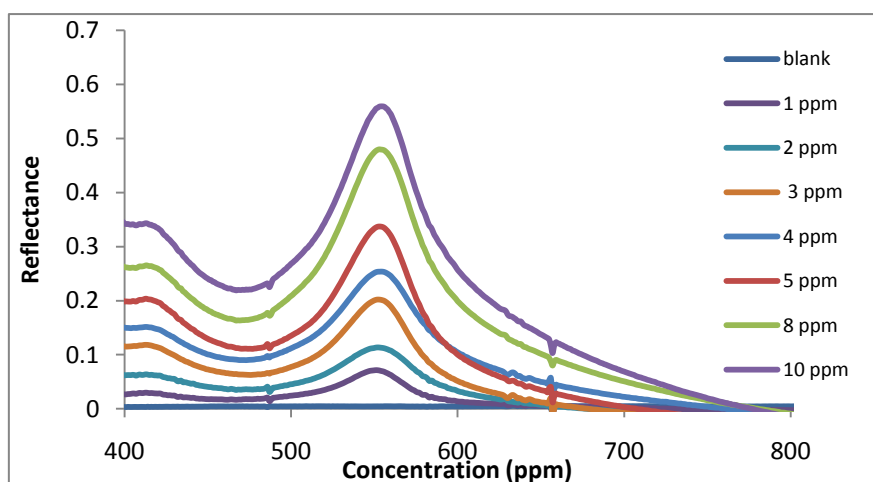
Figure 4.31 The absorbance spectra of gelatin/DMG film that immersed in pH 9 nickel solutions with concentration of 1, 2, 3, 4, 5, 8 and 10 ppm.

Figure 4.32 shows the absorbance of gelatin/DMG films as the function of nickel concentration using the optimized condition for sensor performance. The plot shows a linear correlation between absorbance and nickel concentration in the range of 1-10 ppm.
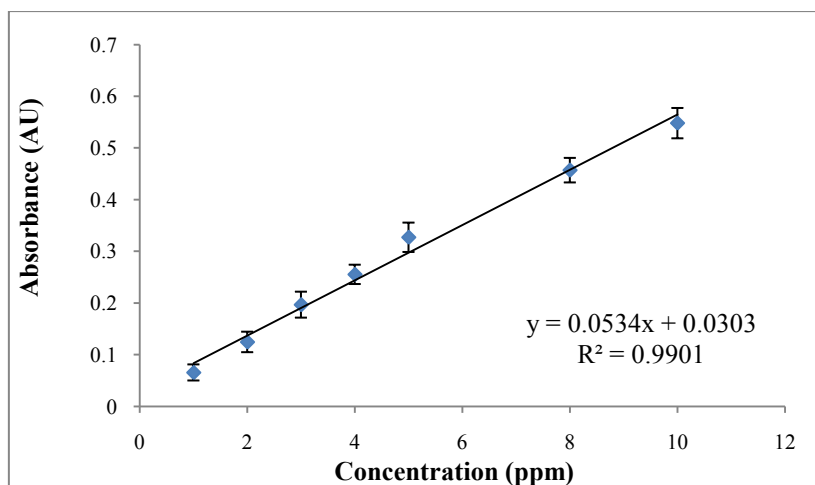
Figure 4.32 Calibration curve for determination of nickel using gelatin/DMG film sensor

4.4.2 Reproducibility

Sensor reproducibility of each sensor format was evaluated by using three sensors independently prepared in each day for 10 days. Each sensor was dipped in a 5 ppm of pH 9 nickel solution for 10 minutes. The response was measured three times. The results were summarized in Table 4.10. The result shows relative standard deviation (R.S.D) of response signal of all sensors: PCL/DMG fiber, PCL/DMG filmand gelatin/DMG film sensor were 2.9%, 2.4 % and 5.1 %, respectively. PCL/DMG sensors show better reproducibility than the gelatin/DMG film. This is might be due to the difficulty in controlling the position of inserted sensor films.

The reproducibility all of three sensors shown the acceptable relative standard deviation when compared with acceptable values of analyte recovery and relative standard deviation of analyte determination that shown in table 4.12.

Table 4.9 The response signal from different sensor tested with 5 ppm nickel solution under optimum condition.

Number of sensor	Mean signal		
	PCL/DMG fiber sensor (Refectance (%) at 547 nm)	PCL/DMG film sensor (Refectance (%) at 550 nm)	Gelatin/DMG film sensor (Absorbance at 550 nm)
1	23.101	26.684	0.334
2	23.237	27.115	0.304
3	22.845	27.387	0.323
4	23.685	27.402	0.349
5	23.993	27.732	0.330
6	23.875	27.709	0.365
7	22.677	27.687	0.349
8	24.878	28.043	0.351
9	23.558	28.554	0.329
10	24.024	28.897	0.346
Mean	23.605	27.721	0.338
SD	0.67	0.65	0.017
% R.S.D	2.9	2.4	5.1

4.4.3 Method validation

The detection performance of these proposed sensors fabricating by both electrospinning and casting methods was validated. In this section, the accuracy and precision of the method were reported in the term of the recovery (%) and relative standard deviation (%), respectively. The detection limit was also determined. The results were summarized in Table 4.10 The results showed that the accuracy and precision of the proposed sensors in nickel determination are acceptable, according to the widely used criteria of analyte recovery and precision at different concentrations (Table 4.11).

Table 4.10 Accuracy, precision and limit of detection of the proposed sensor for nickel determination

Sensor	Ni concentration (ppm)	Recovery (%)[a]	RSD (%)[a]	LOD (ppm)	LOQ (ppm)
PCL/DMG spun fiber sensor	1.0	104.4	6.0		
	5.0	105.0	4.8	0.22	0.97
PCL/DMG film casting sensor	1.0	102.6	7.7		
	5.0	104.7	5.2	0.18	0.89
Gelatin/DMG film casting	1.0	94.0	5.0		
	5.0	97.6	7.4	0.11	0.68

[a] Mean value (n=7)

Table 4.11 Acceptable values of analyte recovery and relative standard deviation of determination of analyte at different concentrations [65]

Analyte (%)	Analyte ratio	Unit	Mean recovery (%)	RSD (%)
100	1	100%	98-102	1.3
10	10^{-1}	10%	98-102	2.8
1	10^{-2}	1%	97-103	2.7
0.1	10^{-3}	0.1%	95-105	3.7
0.01	10^{-4}	100 ppm	90-107	5.3
0.001	10^{-5}	10 ppm	80-110	7.3
0.0001*	10^{-6}	1 ppm	80-110	11
0.00001	10^{-7}	100 ppb	80-110	15
0.000001	10^{-8}	10 ppb	60-115	21
0.0000001	10^{-9}	1 ppb	40-120	30

*Percent analyte that used in this work.

Table 4.12 Comparison of the performance for nickel determinations of optical sensors

Analyte	Analytical procedure	R^2	Detectable range	LOD	Reference
Ni(II)	Optical chemical film sensor; immobilized 2-amino-1-cyclopentene-1-dithiocarboxylic acid on acythl cellulose membrane.	0.9962	0.3-58 ppm	0.03 ppm	[15]
Ni(II))	Colorimetric solid phase extraction: using Dimethylgyloxime as colorimetric reagent.	-	1.8-5 ppm	-	[11]
Ni(II)	Colorimetric solid phase extraction: using Dimethylgyloxime as colorimetric reagent	0.9945	0.5-5 ppm	-	[28]
Ni(II)	Optical chemical sensor; immobilization of 2-(5-bromo-2-pyridylazo)-5-(diethylamino)phenol (Br-PADAP) in Nafion membrane	0.9990	0.5-20 ppm	0.3 ppm	[13]
Ni(II)	Simultaneous preconcentration; using 4-(2-pyridylazo)-resorcinol as ligand and determination by inductively coupled plasma optic emission spectrometry	-	-	6.3 ppb	[66]
	PCL doped with DMG electrospun fiber sensor	0.9925	1-10 ppm	0.22 ppm	-
This work	PCL doped with DMG film casting sensor	0.9964	1-10 ppm	0.18 ppm	-
	Gelatin doped with DMG film casting sensor	0.9921	1-10 ppm	0.11 ppm	-

From Table 4.12, one can be seen that the performance of the proposed sensors was relatively good comparing to the reported methods. The propose method demonstrated a good detection limit that can detect the nickel concentration at the maximum allowable nickel concentration in waste water, it shown in Table 2.1.

4.4.4 Comparison performance of sensors PCL/DMG spun fiber, PCL/DMG film casting and gelatin/DMG film casting sensor

The efficiency of sensor performance of PCL/DMG spun fiber; PCL/DMG film and gelatin/DMG film sensors were compared in terms of linearity, the coefficient of determination and limit of detection of sensor. The results were summarized in Table 4.14. In case of sensor using PCL as media, PCL/DMG film sensors delivered better performance comparing to the electrospun fiber in aspect of the better detection limit and reproducibility with high sensitivity. This result may be due to the different DMG amount on these sensors. PCL/DMG spun fiber is the thinner fiber mats compare to the PCL/DMG film, thus, the less amount of DMG were contained in fibers.

The gelatin/DMG film casting shows lower detection limit compared to the PCL/DMG spun fiber and PCL/DMG film casting sensors because the complexation of $Ni(DMG)_2$ could occur on film surface and inside gelatin film. Moreover, $Ni(DMG)_2$ on gelatin/DMG was detected by absorbance measurement. For absorbance measurement, the light source passed through a sample was detected that mean the both of $Ni(DMG)_2$ on surface and inside gelatin was detected as well. From this reason, the gelatin/DMG film casting presented the high sensitivity than PCL/DMG sensor that measured the $Ni(DMG)_2$ complex only on surface of sensor. However, it delivered lower reproducibility because of absorbance intensity of $Ni(DMG)_2$ on gelatin/DMG had effected by film thickness whereas PCL/DMG sensor did not have effect from film thickness on reflectance measurent. Therefore, the gelatin/DMG and PCL/DMG film casting were used in the real sample application.

Table 4.13 Comparison of linearity equation, the coefficient of determination and limit of detection of PCL/DMG spun fiber, PCL/DMG film casting and Gelatin/DMG film casting sensor

Sensor	Linearity equation	The coefficient of determination, R^2	LOD (ppm)	LOQ (ppm)
PCL/DMG spun fiber sensor	Y=2.0282X+1.1375	R^2=0.9925	0.22	0.97
PCL/DMG film casting sensor	Y=2.0515X+2.7919	R^2=0.9964	0.18	0.89
Gelatin/DMG film casting	Y=0.0534+0.0303	R^2=0.9901	0.11	0.68

4.5 Real sample analysis

The PCL/DMG and gelatin/DMG film casting sensors were applied to determine nickel concentration in real water samples (waste water from jewelry shop and nickel alloys industry) using spiked method. The same sample was parallel tested with inductively coupled plasma-atomic emission spectroscopy (ICP-OES) reference method. These experiments were performed in 5 replicates. The nickel concentration in different water samples were shown in Table 4.14. The results of the proposed sensor presented as percentage of recoveries were shown in Table 4.15.

From Table 4.15, gelatin/DMG and PCL/DMG film casting could detect only nickel in waste water of nickel alloy industrial because the concentration of nickel in Rinsing water from gold line of jewelry industrial and Rinsing water from silver line of jewelry industrial lees than detection limit of these sensors. The static t-test was use to compare the concentration means of nickel in real water sample obtained from the proposed sensor and ICP-OES. The results shown the $t_{critical}$ = 2.77 and $t_{statistic}$ = 0.28 and -0.27 0f PCL/DMG and gelatin/DMG film casting, respectively. This result showed the $t_{statistic}$ less than $t_{critical}$, thus, no significant different value of both methods.

Table 4.14 The comparison results of gelatin/DMG, PCL/DMG film casting and ICP-OES for determination of nickel ions in real sample

Water sample (mg/L)	PCL/DMG casted film		gelatin/DMG casted film		Reference method
	Found[a] (ppm)	t-statistic ($t_{0.05,5}$=2.77)	Found[a] (ppm)	t-statistic ($t_{0.05,5}$=2.77)	ICP-OES (ppm)
Rinsing water from gold line of jewelry industrial	n.d	n.d	n.d	n.d	0.05±0.01
Rinsing water from silver line of jewelry industrial	n.d	n.d	n.d	n.d	0.08±0.01
waste water of nickel alloy industrial	9.9±0.2	0.28	9.6±0.3	-0.27	9.79±0.28

n.d. = Non detectable, [a] Mean value of five determination

Table 4.15 Determination of nickel in real water samples

Sample	Added (mg L^{-1})	Found[a] (ppm)			Recovery (%)		
		PCL film	gelatin film	ICP-OES	PCL film	gelatin film	ICP-OES
Rinsing water from gold	0.7	0.8±0.20	0.7±0.02	0.8±0.01	106.9	87.8	105.9
line of jewelry industrial	1.0	1.1±0.09	1.0±0.03	1.1±0.01	107.4	93.4	102.5
	5.0	5.2±0.02	4.8±0.011	5.1±0.01	101.9	104.8	100.4
Rinsing water from	0.7	0.7±0.06	0.7±0.02	0.8±0.01	88.4.1	88.3	105.0
silver line of jewelry	1.0	1.0±0.07	1.0±0.03	1.1±0.01	94.1	96.2	102.7
industrial	5.0	4.9±0.10	5.3±0.11	5.1±0.01	95.7	96.9	100.3
waste water of nickel	0.7	1.6±0.04	1.6±0.02	1.7±0.01	92.7	92.8	103.4
alloy industrial	1.0	2.0±0.05	1.9±0.02	2.0±0.01	100.5	93.7	102.2
	5.0	6.2±0.06	6.2±0.11	6.0±0.08	104.7	104.0	100.1

[a] Mean ± SD (n=5)

The recoveries of nickel from spiked samples with Ni standard of three concentration levels (0.7, 1 and 5 ppm) are acceptable, according t analyte recovery and precision at different concentrations (Table 4.11). The values obtained from the proposed method (ICP-OES) were not significantly different. Therefore, the proposed method can be applied for the determination of nickel in water samples with acceptable accuracy

CHAPTER V

CONCLUSION

The optical sensor for determination nickel(II) ions in water sample was fabricated in three formats: PCL doped with DMG electrospun fiber, PCL doped with DMG film cast and gelatin doped with DMG filmscast. The sensor response to nickel (II) ions was occurred by forming the red-pink complex of $Ni(DMG)_2$ after dipping in different concentration of nickel.

For PCL doped with DMG electrospun fiber, PCL/DMG solutions were spun at the electrical potential of 20 kV, the working distance of 20 cm, and a flow rate of 1.2 mL/h. With the increasing the amount of DMG, the effect of added DMG on the fiber size was found to be small. ATR-FTIR analysis indicated that the interaction between PCL and DMG was weak. PCL/DMG blend fibers in mass ratio of 80:20 with diameters 275 ± 39 nm have been successfully produced by using the electrospinning process. The suitable solvent for used in this experiment was DMF/DCM (50/50). Furthermore, PCL/DMG blend fibers have been successfully used as nickel sensing.

For PCL doped with DMG film cast, PCL/DMG solution were casted and produced the porous surface with porous diameter 6.48 ± 2.04 μm of PCL/DMG blend film in mass ratio of 80:20. The FT-IR of PCL/DMG film cast showed the similar spectrum to PCL/DMG electrospun fibers this due to the similarity of chemical structure of film and fiber. It was indicated that these two components were simply blended.

For gelatin/DMG film cast that is hydrophilic polymer suport, it showed different characteristic sensor poperties; transparence film and detect $Ni(DMG)_2$ forming by measuring the absorbance sigmal of both of film and solution. At the mass ratio of gelatin/DMG of 96.4 : 3.6 delivered the uniform film surface and good performance for nickel determination; high absorbance intensity of $Ni(DMG)_2$ and small standard deviation. The prepared gelatin/DMG film were shown the detection

for nickel(II) ions in the concentration with a good linear response between 1-10 ppm under optimum condition.

All of the analytical parameters of the optimized sensors used for determination of nickel(II) were summarized in Table 5.1.

Table 5.1 The summarize of analytical parameters of the optimized sensors used for determination of nickel (II) ion.

Parameters	Measurement value		
	PCL/DMG electrospun fiber	PCL/DMG film cast	Gelatin film cast
Mass ratio of PCL/DMG	80:20	80:20	96.4:3.6
pH of nickel solution	8-9	8-9	9
Response time (minute)	10	10	10
Interfering ion when present at equal concentration of Ni $^{2+}$	Co^{2+}, Fe^{3+} and Pb^{2+}	Co^{2+}, Fe^{3+} and Pb^2	Co^{2+}, Cu^{2+}, Fe^{3+} and Pb^2
Linear range (ppm)	1-10	1-10	0.8-10
Reproducibility (% R.S.D, n=10)	2.9	2.4	5.1
Precision (% R.S.D., n=7)	4.8 (Ni 1ppm) 6.0 (Ni 5ppm)	5.2(Ni 1ppm) 7.7(Ni 5ppm)	5.0 (Ni 1ppm) 7.4 (Ni 5ppm)
Accuracy (Recovery, n=7)	104.4(Ni 1ppm) 105.0(Ni 5ppm)	102.6(Ni 1ppm) 104.7(Ni 5ppm)	94.0 (Ni 1ppm) 97.6 (Ni 5ppm)

Table 5.1 The summarized of analytical parameters of the optimized sensors used for determination of nickel(II) (Cont.)

Parameters	Measurement value		
	PCL/DMG electrospun fiber	PCL/DMG film cast	Gelatin film cast
LOD (ppm, n=20)	0.22	0.18	0.11
LOQ (ppm, n=20)	0.97	0.89	0.68
Real sample of waste water of nickel alloy industrial compared with ICP-OES (9.79$\pm$0.28 ppm)	-	9.9$\pm$0.2	9.6$\pm$0.3

Finally, this proposes method was successfully applied for the determination of nickel ions in water samples. It was suitable for used to pre-screen nickel in water sample and in the filed under the maximum nickel concentration in wastewater guidelines and regulations of the Ministry of Science Natural Resources. Because of it showed the simple detection method, dipping sensor in solution. However, the interference ions is the large problem of the propose method.

Suggestions for future work

From the problem of this method is interference ions, the suggestion for the further work should to be find method that can eliminate these interfere ions such as added the masking agent in to sensor, removed the interference ions before used. Moreover, the propose sensor should be developed to naked-eye or test kit which easy to use in flied.

REFERENCES

[1] Wikipedia. Nickel. [Online]. Available from: *http://en.wikipedia.org/wiki/Nickel.* [2011, January 9].

[2] Agency for Toxic Substances and Disease Registry. Public Health statement of nickel. 2005; Available from: *http://www.atsdr.cdc.gov/ToxProfiles/tp15-c1-b.pdf.* [2011, January 9].

[3] Ministry of Natural Resources and Environment. Water Quality standards from industrial 2009; Available from: *http://www.deqp.go.th/upload/schemaID%5B52%5D/standard.ppt#257 ,1,Slide.* [2011, January 9]

[4] Xie, F.Z., et al., *Solid phase extraction of lead (II), copper (II), cadmium (II) and nickel (II) using gallic acid-modified silica gel prior to determination by flame atomic absorption spectrometry.* Talanta, 2008. **74**(4): p. 836-843.

[5] Karami, H., et al., *On-line preconcentration and simultaneous determination of heavy metal ions by inductively coupled plasma-atomic emission spectrometry.* Analytica Chimica Acta, 2004. **509**(1): p. 89-94.

[6] Munoz, E., S. Palmero, and M.A. Garcia-Garcia, *A continuous flow system design for simultaneous determination of heavy metals in river water samples.* Talanta, 2002. **57**(5): p. 985-992.

[7] Yari, A. and N. Afshari, *An optical copper(II)-selective sensor based on a newly synthesized thioxanthone derivative, 1-hydroxy-3,4-dimethylthioxanthone.* Sensors and Actuators B-Chemical, 2006. **119**(2): p. 531-537.

[8] Alizadeh, A., et al., *Rapid and selective lead (II) colorimetric sensor based on azacrown ether-functionalized gold nanoparticles.* Nanotechnology. **21**(31): p. 8.

[9] Li, J., et al., *A highly selective fluorescent sensor for Hg2+ based on the water-soluble poly(p-phenyleneethynylene).* Polymer. **51**(15): p. 3425-3430.

[10] Motlagh, M.G., M.A. Taher, and A. Ahmadi, *PVC membrane and coated graphite potentiometric sensors based on 1-phenyl-3-pyridin-2-yl-thiourea for selective determination of iron(III).* Electrochimica Acta. **55**(22): p. 6724-6730.

[11] Gazda, D.B., J.S. Fritz, and M.D. Porter, *Multiplexed colorimetric solid-phase extraction: Determination of silver(I), nickel(II), and sample pH.* Analytical Chemistry, 2004. **76**(16): p. 4881-4887.

[12] Fritz JS, A.M., S. A. Steiner, and M. D. Porter, *Rapid determination of ions by combined solid-phase extraction--diffuse reflectance spectroscopy.* J Chromatogr A, 2003. **997**(16): p. 41-50.

[13] Amini, M.K., et al., *Development of an optical chemical sensor based on 2-(5-bromo-2-pyridylazo)-5-(diethylamino)phenol in Nafion for determination of nickel ion.* Talanta, 2004. **63**(3): p. 713-720.

[14 Hashemi, P., et al., *High sensitive optode for selective determination of Ni2+ based on the covalently immobilized thionine in agarose membrane.* Sensors and Actuators B: Chemical, 2010. **153**(1): p. 24-28.

[15] Ensafi, A.A. and M. Bakhshi, *New stable optical film sensor based on immobilization of 2-amino-1-cyclopentene-1-dithiocarboxylic acid on acetyl cellulose membrane for Ni(II) determination.* Sensors and Actuators B: Chemical, 2003. **96**(1-2): p. 435-440.

[16] Huang, Z.-M., et al., *A review on polymer nanofibers by electrospinning and their applications in nanocomposites.* Composites Science and Technology, 2003. **63**(15): p. 2223-2253.

[17] Timothy H. Grafe, K.M.G., *Nanofiber Webs from Electrospinning* in *Fifth International Conference* 2003 Stuttgart, Germany p. 5.

[18] Rutledge, G.C. and S.V. Fridrikh, *Formation of fibers by electrospinning.* Advanced Drug Delivery Reviews, 2007. **59**(14): p. 1384-1391.

[19] Armstrong, K.C., et al., *Individual and simultaneous determination of lead, cadmium, and zinc by anodic stripping voltammetry at a bismuth bulk electrode.* Talanta. **82**(2): p. 675-680.

[20] Mayr, T., *Optical Sensors for the Determination of Heavy Metal Ions*, in *Chemistry*. 2002, Regensburg: Regensburg. p. 140.

[21] Steinberg, I.M., A. Lobnik, and O.S. Wolfbeis, *Characterisation of an optical sensor membrane based on the metal ion indicator Pyrocatechol Violet.* Sensors and Actuators B: Chemical, 2003. **90**(1-3): p. 230-235.

[22] Kuswandi, B., *Optical Chemical Sensors for the Determination of Heavy Metal Ions: A mini review. Jurnal ILMU DASAR, 2000. **1**(2): p. 18 - 29.*

[23] Oehme, I. and O.S. Wolfbeis, *Optical sensors for determination of heavy metal ions.* Microchimica Acta, 1997. **126**(3): p. 177-192.

[24] Janzen, M.C., et al., *Colorimetric Sensor Arrays for Volatile Organic Compounds.* Analytical Chemistry, 2006. **78**(11): p. 3591-3600.

[25] Jeronimo, P.C.A., et al., *Colorimetric bismuth determination in pharmaceuticals using a xylenol orange sol-gel sensor coupled to a multicommutated flow system.* Analytica Chimica Acta, 2004. **504**(2): p. 235-241.

[26] Guclu, K., et al., *A combined spectrophotometric-AAS method for the analysis of trace metal, EDTA, and metal-EDTA mixture solutions in adsorption modeling experiments.* Talanta, 2000. **53**(1): p. 213-222.

[27] Svehla, G., *Vogel's Qualitative Inorganic Analysis*. 7th ed. 1996: Prentice Hall. 360.

[28] Gazda, D.B., J.S. Fritz, and M.D. Porter, *Determination of nickel(II) as the nickel dimethylglyoxime complex using colorimetric solid phase extraction.* Analytica Chimica Acta, 2004. **508**(1): p. 53-59.

[29] Carter, E.S. and K.H. Dahmen, *Nickel determination by complexation utilizing a functionalized optical waveguide sensor.* Abstracts of Papers of the American Chemical Society, 2001. **221**: p. 477-INOR.

[30] Korposh, S.O., et al., *Matrix influence on the optical response of composite bacteriorhodopsin films to ammonia.* Sensors and Actuators B: Chemical, 2008. **133**(1): p. 281-290.

[31] Malcik, N., et al., *Immobilised reagents for optical heavy metal ions sensing.* Sensors and Actuators B: Chemical, 1998. **53**(3): p. 211-221.

[32] Oter, O., et al., *Photocharacterization of a novel fluorescent Schiff Base and investigation of its utility as an optical Fe3+ sensor in PVC matrix.* Dyes and Pigments, 2007. **74**(3): p. 730-735.

[33] Lepore, M., et al., *Glucose concentration determination by means of fluorescence emission spectra of soluble and insoluble glucose oxidase: some useful indications for optical fibre-based sensors.* Journal of Molecular Catalysis B: Enzymatic, 2004. **31**(4-6): p. 151-158.

[34] GEA Process Engineering Inc [online]. Spray dring blood and gelatin (animal). Available from: *http://www.niroinc.com/food_chemical/spray_drying_gelatin.asp.* [2011, march 4]

[35] Li, B., et al., *Quick dissolvable, edible and heatsealable blend films based on konjac glucomannan - Gelatin.* Food Research International, 2006. **39**(5): p. 544-549.

[36] Tang, Z.G., et al., *Surface properties and biocompatibility of solvent-cast poly[[var epsilon]-caprolactone] films.* Biomaterials, 2004. **25**(19): p. 4741-4748.

[37] Nakagawa, K., et al., *Development of an eco-friendly optical sensor element based on tetraphenylporphyrin derivatives dispersed in biodegradable polymer: Effects of substituents of tetraphenylporphyrins on HCl detection and biodegradation.* Sensors and Actuators B: Chemical, 2005. **108**(1-2): p. 542-546.

[38] Wikipedia. Polycaprolactone. [Online]. Available from: *http://en.wikipedia.org/wiki/Polycaprolactone.* [2010, November 17]

[39] Mirabella, F.M., *Modern techniques in applied molecular spectroscopy* II. 1998, Newyork: John Wiley & Sons, Inc. 186-208.

[40] Andrady, A.L., *Science and technology of Polymer Nanofibers.* 2008, New Jesey: Wiley. 403.

[41] Sautter, B.P., *Continuous Polymer Nanofibers Using Electrospinning,* in *Mechanical Engineering.* 2005, University of Illinois at Chicago: Chicago. p. 29.

[42] Deitzel, J.M., et al., *The effect of processing variables on the morphology of electrospun nanofibers and textiles.* Polymer, 2001. **42**(1): p. 261-272.

[43] Electrospinning. [Online] Available from: *http://www.che.vt.edu/Wilkes/electrospinning/electrspinning.html.* [2010, July 15]

[44] Yusof, N.A. and M. Ahmad, *A flow-through optical fibre reflectance sensor for the detection of lead ion based on immobilised gallocynine.* Sensors and Actuators B: Chemical, 2003. **94**(2): p. 201-209.

[45] Xiang, Y., et al., *Highly sensitive and selective optical chemosensor for determination of Cu2+ in aqueous solution.* Talanta, 2008. **74**(5): p. 1148-1153.

[46] Ozlem Oter a, K.E.a., *, Rafet Kılıncarslan b, Mahmut Ulusoy b, Bekir Cetinkaya, *Photocharacterization of a novel fluorescent Schiff Base and investigation of its utility as an optical Fe3þ sensor in PVC matrix.* Dyes and Pigments, 2007. **74**: p. 730e735.

[47] Ensafi, A.A. and A. Aboutalebi, *A versatile stable cobalt optical sensor based on pyrogallol red immobilization on cellulose acetate film.* Sensors and Actuators B: Chemical, 2005. **105**(2): p. 479-483.

[48] Sands, T.J., et al., *A highly versatile stable optical sensor based on 4-decyloxy-2-(2-pyridylazo)-1-naphthol in Nafion for the determination of copper.* Sensors and Actuators B: Chemical, 2002. **85**(1-2): p. 33-41.

[49] Guo, L., et al., *An organically modified sol-gel membrane for detection of lead ion by using 2-hydroxy-1-naphthaldehydene-8-aminoquinoline as fluorescence probe.* Sensors and Actuators B: Chemical, 2008. **130**(2): p. 789-794.

[50] Hashemi, P., et al., *A calmagite immobilized agarose membrane optical sensor for selective monitoring of Cu^{2+}.* Sensors and Actuators B: Chemical, 2008. **129**(1): p. 332-338.

[51] Radloff, D., et al., *Stability improvement of an optochemical heavy metal ion sensor by covalent receptor binding.* Sensors and Actuators B: Chemical, 1996. **35**(1-3): p. 207-211.

[52] Ressalan, S. and C.S.P. Iyer, *Absorption and fluorescence spectroscopy of 3-hydroxy-3-phenyl-1-o-carboxyphenyltriazene and its copper (II), nickel*

(II) and zinc (II) complexes: a novel fluorescence sensor. Journal of Luminescence, 2005. **111**(3): p. 121-129.

[53] Hashemi, P., et al., *High sensitive optode for selective determination of Ni2+ based on the covalently immobilized thionine in agarose membrane.* Sensors and Actuators B: Chemical, 2011. **153**(1): p. 24-28.

[54] Merck. Nickel Test. [online] 2011; Available from: *http://www.merck-chemicals.com.* [2011, march 2]

[55] Ratanavaraporn, J., et al., *Influences of physical and chemical crosslinking techniques on electrospun type A and B gelatin fiber mats.* International Journal of Biological Macromolecules, 2010. **47**(4): p. 431-438.

[56] Han, J., C.J. Branford-White, and L.-M. Zhu, *Preparation of poly([epsilon]-caprolactone)/poly(trimethylene carbonate) blend nanofibers by electrospinning.* Carbohydrate Polymers, 2010. **79**(1): p. 214-218.

[57] Lacroix, S., et al., *Physicochemical Properties of Alginate/Polycaprolactone-Based Films Containing Essential Oils.* journal of Agricultural and Food Chemistry, 2006. **54**: p. 10205-10214.

[58] Panja, P.K., et al., *Infrared spectroscopic studies of dimethylglyoxime chelates of nickel, cobalt, copper, palladium and platinum.* Journal of Molecular Structure, 1991. **249**(2-4): p. 277-283.

[59] Chyan, T., et al., *Detection of Ni2+ by a Dimethylglyoxime Probe Using Attenuated Total-Reflection Infrared Spectroscopy.* Analytical Sciences, 2002. **18**(4): p. 449.

[60] Kunal Pal, A.K.B., and Dipak K. Majumdar, *Preparation and Characterization of Polyvinyl Alcohol–Gelatin Hydrogel Membranes for Biomedical Applications.* PharmSciTech, 2007. **1**(8).

[61] Muyonga, J.H., C.G.B. Cole, and K.G. Duodu, *Fourier transform infrared (FTIR) spectroscopic study of acid soluble collagen and gelatin from skins and bones of young and adult Nile perch (Lates niloticus).* Food Chemistry, 2004. **86**(3): p. 325-332.

[62] Yannas, I.V. and A.V. Tobolsky, *Cross-linking of Gelatine by Dehydration.* Nature, 1967. **215**(5100): p. 509-510.

[63] Haugh, M.G., M.J. Jaasma, and F.J. O'Brien, *The effect of dehydrothermal treatment on the mechanical and structural properties of collagen-GAG scaffolds.* Journal of Biomedical Materials Research Part A, 2009. **89A**(2): p. 363-369.

[64] Mark, R. L. *Validation and qualification in analytical laboratories.* Illinois, Interpharm Press, 1999

[65] Silva, E.L., P.d.S. Roldan, and M.F. Giné, *Simultaneous preconcentration of copper, zinc, cadmium, and nickel in water samples by cloud point extraction using 4-(2-pyridylazo)-resorcinol and their determination by inductively coupled plasma optic emission spectrometry.* Journal of Hazardous Materials, 2009. **171**: p. 1133-1138.

[66] Marczenko, Z., *Spectrophotometric determination of elements.* 1976, New York: Wiley.

VITA

Miss Thanyapan Poltue was born on September 10, 1984 in Kalasin, Thailand. She received her Bachelor's degree of Science in chemistry from KhonKean University in 2007. After that, she has been a graduate student at the Department of Chemistry, Chulalongkorn University and become a member of Chromatography and Separation Research Unit under the supervision of Dr. Luxsana Dubas. She finished her Master's degree of Science in 2011. Her present address is 223/3 Bhurapa road, Huayphung District, Kalasin, Thailand, 46240. Contact number is 089-4498341. Email: thanya_toto@hotmail.com.